LE

6/4

NASA Technical Paper 2597

May 1986

Design of 9.271-Pressure-Ratio Five-Stage Core Compressor and Overall Performance for First Three Stages

Ronald J. Steinke

NASA

NASA
Technical
Paper
2597

1986

Design of 9.271-Pressure-Ratio Five-Stage Core Compressor and Overall Performance for First Three Stages

Ronald J. Steinke

Lewis Research Center
Cleveland, Ohio

National Aeronautics
and Space Administration

**Scientific and Technical
Information Branch**

Summary

This paper reports Lewis-conducted basic research for advanced compressor systems. The primary objectives were (1) to experimentally assess stages in a multistage environment and (2) to establish the current level of technology attainable in axial stage groups with high tip speed, high stage loading, and low aspect ratio.

An aerodynamic design is presented for a five-stage core compressor with a 9.271 pressure ratio and 29.710 kg/sec flow rate. The inlet tip speed for the first stage rotor is 430.291 m/sec, and the inlet specific flow is 193.173 kg/m^2 sec. For the first three stages of this five-stage core compressor, an additional aeromechanical design was completed. This inlet three-stage group was fabricated and evaluated experimentally. The inlet stage group is representative of that of an advanced high-speed, high-pressure-ratio core compressor. At design speed and IGV-stator setting angles a three-dimensional Euler code successfully predicted the experimentally measured flow that was 9.1 percent higher than design. At all speeds measured adiabatic efficiency improved for an optimal IGV-stator reset schedule that was determined by an optimization code.

Introduction

An experimental program was undertaken by the Lewis Research Center on fans and compressors for advanced air-breathing engines to assess and improve the technology needed for high pressure ratio, good efficiency, and adequate stall margin in as few stages as possible. The core compressor in an advanced turbofan engine is a prime component of the engine and has a large effect on engine performance and efficiency. The high turbine inlet temperatures of advanced engines lead to optimum thermodynamic cycles that require high overall pressure ratios of about 40:1. The core compressor component must efficiently produce about 80 percent of this pressure rise.

Several core compressors have been designed for the evaluation of changes in tip speed, reaction, etc. The core compressors consist of base cores and rebladed cores. The rebladed cores were obtained from existing base-core hardware along with new blades.

For high-speed, high-pressure-ratio core compressors of good efficiency and range, the inlet stage groups must efficiently produce the desired pressure ratio and flow distribution for the succeeding stages. This requires good stage matching of the inlet group stages.

This report presents (1) the overall aerodynamic design for a core compressor designated 74A and (2) the blade-element aerodynamic and mechanical design details and experimental overall performance for the core's inlet stage group which consist of the inlet guide vanes (IGV) and the first three stages. Core compressor 74A has five stages and is designed for a 9.271:1 pressure ratio and 29.710-kg/sec flow. At the rotor 1 inlet tip speed was 430.291 m/sec, annular flow was 193.173 kg/sec m^2, and hub to tip radius ratio was 0.488. The inlet stage group had a design pressure ratio of 4.474 and design efficiency of 0.799.

The core 74A inlet stage group was tested in the Lewis multistage compressor test facility. The compressor's IGV and stator blade setting angles were variable and reoriented to achieve maximum overall adiabatic efficiency, using a vane reset optimization computer code. Experimental results, for both design and optimum IGV-stator settings, are presented over the stable operating range at rotative speeds from 60 to 100 percent of design.

Pertinent symbols and equations are in appendix A and B. The abbreviations used in the computer generated design tables are defined in appendix C.

Aerodynamic Design

The computer code of reference 1 was used for both the compressor aerodynamic design and the blading coordinate specifications. The aerodynamic solution provides velocity diagrams on selected streamlines of revolution at the blade row edges. Steady axisymmetric flow is assumed, and the aerodynamic solution is for the two-dimensional flow field in the meridional plane. The computer code obtains solutions to the equations of motion which neglect blade forces and are only valid for calculating stations outside blade rows. The streamline curvatures are computed from spline curve fits through calculated streamline locations for each station.

Blading is defined from stacked, blade elements associated with each streamline. For each blade element the inlet and outlet angles are obtained from empirical incidence and deviation-angle adjustments to the relative flow angles of the computed velocity diagrams. The blade elements are defined and stacked within the aerodynamic solution interation so that the velocity diagrams can be computed at the blade edges.

The input to the design code consist of flow-path geometry, overall total pressure ratio, mass flow, rotative speed, distribution of energy per stage, blade geometry, and axial location of blade rows in the flowpath. The output includes (1) overall design point summary for the compressor and each blade row, (2) blade-element parameters for each blade row, and (3) coordinates for plane sections through the blades that are convenient for manufacturing purposes.

The aerodynamic design details are discussed in this section under various subheadings to allow the reader to readily locate the discussion about a particular design parameter.

Flowpath

The selected flowpath geometry was based on the following considerations: (1) blade loading level, (2) overall and local meridional velocity diffusion, and (3) compressor mass flow.

The flow path with blades for compressor 74A is shown in figure 1. The flow path's mean radius increases with increased axial distance. This increase tends to reduce the drop in mean-corrected rotor-wheel speed for downstream stages, which reduces downstream blade loading. Flowpath hub radius increased smoothly between compressor inlet and outlet. Tip radius sharply decreased across the rotors. This caused tip flowpath curvature, as viewed from the rotational axis, to be

Tip axial coordinates, cm	Tip radius, cm	Hub axial coordinates, cm	Hub radius, cm
-12.733	25.654	-12.733	9.728
-5.113	25.654	-5.113	10.986
1.237	25.654	-.033	12.497
1.999	25.603	2.507	13.411
2.507	25.552	5.047	14.224
3.777	25.324	7.587	14.986
5.047	25.070	10.127	15.687
5.936	24.943	12.667	16.337
8.476	24.790	14.572	16.789
14.445	24.765	17.112	17.297
15.207	24.676	19.779	17.793
15.778	24.575	23.078	18.337
16.477	24.460	25.237	18.644
17.493	24.301	27.920	18.999
19.779	24.194	29.952	19.253
23.081	24.194	32.131	19.520
24.732	24.130	34.036	19.736
25.113	24.067	35.745	19.926
25.603	24.003	38.067	20.155
26.637	23.813	40.777	20.371
27.272	23.736	41.877	20.422
30.574	23.660	43.147	20.472
31.387	23.660		
32.352	23.660		
32.987	23.622		
33.409	23.559		
34.003	23.457		
34.511	23.419		
35.908	23.393		
37.254	23.381		
39.218	23.287		
39.464	23.261		
39.718	23.223		
39.896	23.198		
40.607	23.175		
43.147	23.101		

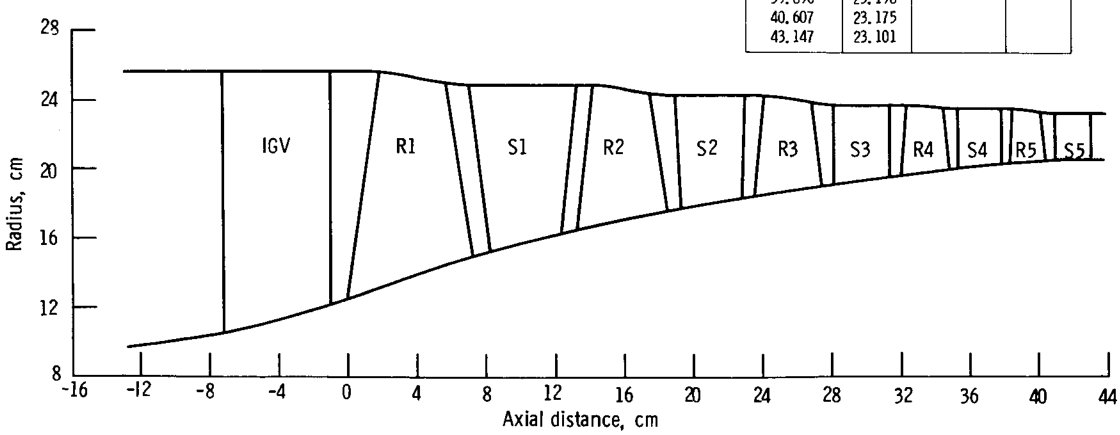

Figure 1.—Flowpath for compressor 74A.

concave at each rotor inlet and convex at each rotor outlet. For each rotor tip region the resulting axial distribution of tip flow-path curvature reduced tip region velocity diffusion and, hence, rotor blade loading.

For the three-stage configuration of compressor 74A, the flowpath was altered downstream of stator 3 (fig. 2). The annulus downstream of stator 3 was modified to maintain similar design flow conditions at the stator 3 outlet. Design static-pressure distributions at the stator 3 outlet are shown in figure 3 for both the three- and five-stage configurations. These static pressures match within experimental data measurement accuracy.

Blade spacing.—Axial spacing in research compressors is often a compromise between (1) the large blade row spacing needed for reliable interstage survey instrumentation and (2) close coupled blade rows of typical flight engine compressors. Since the emphasis was on good efficiency and range, close-coupled blade rows were selected to avoid the losses associated with large blade row spacing.

For a constant aerodynamic chord, axial spacing is higher in the tip region than the hub region, because rotor setting angle increases with radius. Thus, for a given axial length, either rotor or stator tip chord can be increased to reduce tip blade loading. For stators 1 and 2 tip chord was increased

Tip axial coordinates, cm	Tip radius, cm	Hub axial coordinates, cm	Hub radius, cm
-12.733	25.654	-12.733	9.728
-5.113	25.654	-5.113	10.986
1.237	25.654	-.033	12.497
1.999	25.603	2.507	13.411
2.507	25.552	5.047	14.224
3.777	25.324	7.587	14.986
5.047	25.070	10.127	15.687
5.936	24.943	12.667	16.337
8.476	24.790	14.572	16.789
14.445	24.765	17.112	17.297
15.207	24.676	19.779	17.793
15.778	24.575	23.078	18.337
16.477	24.460	25.237	18.644
17.493	24.301	27.920	18.999
19.779	24.194	29.952	19.253
23.081	24.194	32.131	19.322
24.732	24.130	34.036	19.441
25.113	24.067	35.746	19.482
25.603	24.003	38.067	19.507
26.637	23.813	40.777	19.507
27.272	23.736	41.877	19.507
30.574	23.660	43.147	19.512
31.387	23.660		
32.352	23.660		
32.987	23.658		
33.409	23.658		
34.003	23.658		
34.511	23.658		
35.908	23.658		
37.254	23.658		
39.218	23.658		
39.464	23.658		
39.718	23.658		
39.896	23.658		
40.607	23.658		
43.147	23.658		

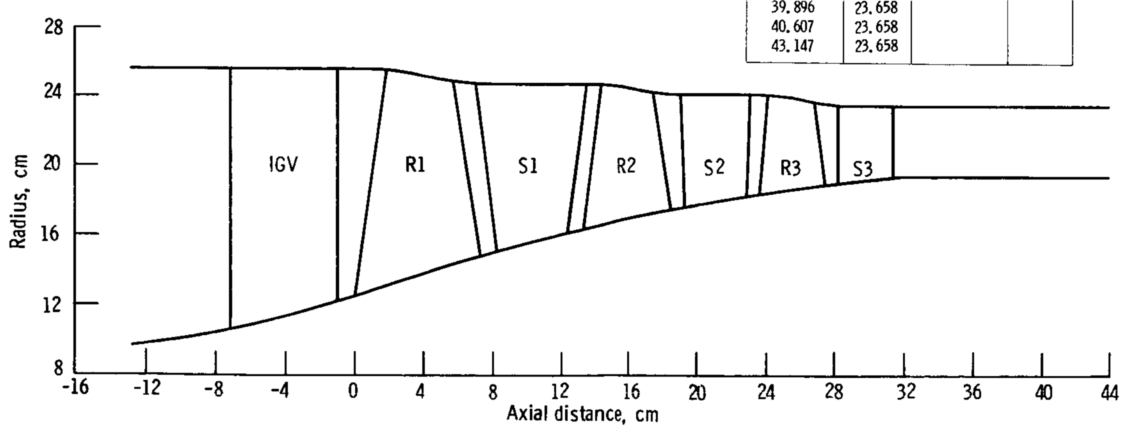

Figure 2.—Flowpath for inlet stage group of compressor 74A.

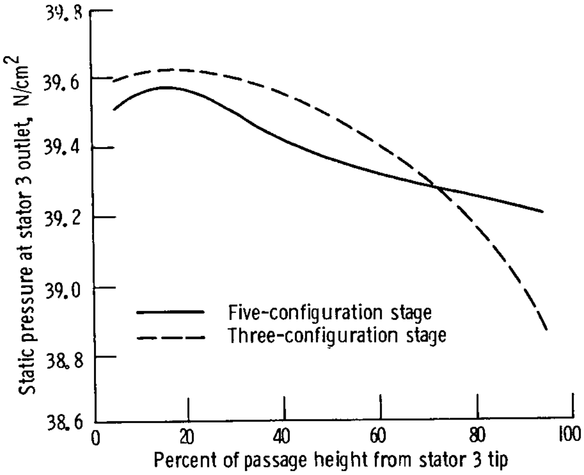

Figure 3.—Design static pressures at stator 3 trailing edge.

because stator tip loading is much higher than rotor tip loading and because the stator tip must operate over a wide range of incidence angles and loading when the rotor operates off design.

Blade aspect ratio.—In the selection of blade aspect ratio, the following were considered: (1) part span dampers, (2) solidity (enough to allow high blade loading levels), (3) rotor-stator chord requirements per stage, and (4) axial compressor length.

The selected aspect ratio, solidity, and number of blades are listed in table I for each blade row. The blade aspect ratios were low enough to eliminate the need for rotor part-span dampers. The selected low-aspect-ratio, moderate solidity blading allowed high loading or pressure rise per stage. Therefore, fewer blades and stages were required to achieve the overall pressure ratio.

For a stage where the rotor and stator loading are about equal, the rotor tended to require more flow guidance or blade chord to achieve efficient blade loading. For each stage the rotor aspect ratio was lower than the corresponding stator aspect ratio. The inequality of rotor and stator aspect ratios for each stage was expected to give better performance than a similar stage having equal rotor and stator aspect ratios.

Flow blockage.—To properly match the stages flow blockage is applied to the annular flow throughout the flow field. The flow blockage is associated with end-wall boundary layers, blade thickness, blade wakes, and secondary flow. The blockage factor for compressor 74A, expressed as a fraction of local annular area, was equally applied to the flow-path hub and tip. Total blockage (see fig. 4) increases from 0.04 at the rotor 1 inlet to 0.14 at the stator 5 outlet.

Velocity Diagrams

Reaction.—The individual stage reaction level is set by the rotor inlet design absolute flow angle. Positive inlet absolute flow angle (preswirl) causes the stage reaction level to decrease. Stage preswirl unloads selected rotor blade elements

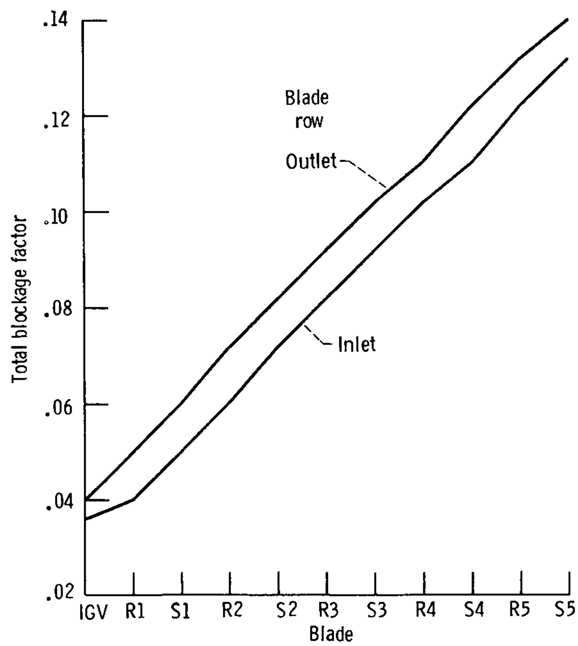

Figure 4.—Total blockage factors applied to flowpath.

or reduces the inlet relative Mach number at selected rotor elements. When preswirl is used, the stator loading and stator inlet absolute Mach number usually increase.

No preswirl was used for compressor 74A. The reaction (the ratio of rotor to stage static pressure) was high (greater than 0.85) for all stages.

Axial energy distribution.—In a multistage compressor, consideration is given to both the axial and radial energy distribution. Good energy distribution is important to the efficiency of a wide range of compressor operations.

During operation along a constant speed line, a multistage compressor tends to pivot about its middle stages with the inlet and outlet stages forced into off-design operation. Generally, a stage designed for low blade loading or energy addition has a wider range of efficient operation than a stage designed for a high energy addition. Therefore, the axial energy addition for compressor 74A is highest for the stage 3 and lowest for stages 1 (inlet) and 5 (outlet). Figure 5 shows the selected stage energy addition expressed as the fraction of total compressor energy addition.

Radial energy distributions.—For each stage the radial energy distribution is determined from its rotor energy input. The radial energy distribution is typically selected to alleviate high blade-element loading on a some particular blade row for some portion of the blade span. If the whole blade row span is under high loading, an adjustment to the compressor axial energy distribution may be needed to reduce the loading.

For compressor 74A the blade exit radial energy distribution was set by the specification of radially constant total pressure distributions at the rotor exits. The total pressure ratio of a rotor blade element, therefore, must compensate for pressure losses from the preceeding stator blade element. Thus,

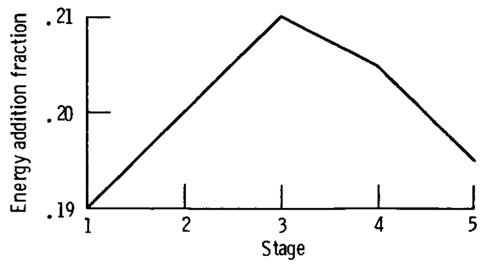

Figure 5.—Axial energy addition fraction per stage.

both rotor and stator radial loss gradients contribute to radial gradients in rotor energy addition. Generally, the higher end-wall blade losses result in higher energy addition in the rotor hub and tip regions.

Loss Model

The loss model is based on correlations from relevant experimental data for single stages with blading which is similar to the blading of compressor 74A. The two correlations, profile loss and shock loss, are based on the data from references 2 to 11. Loss correlations were applied to all blading of 74A except the inlet guide vanes (IGV). For the IGV's, a radially constant 2 percent drop in total pressure is used.

Profile losses.—Profile losses were based on a correlation that relates the total-pressure profile loss parameter to diffusion factor and percent of blade span (ref. 12). With the data of references 2 to 11 used as input, separate profile loss correlations were obtained for rotors and stators (see figs. 6 and 7). The loss correlations indicated the following trends: (1) profile losses increase with increasing blade loading diffusion factor and (2) generally, for a constant diffusion factor value, profile losses are highest in the blade hub and tip regions.

Shock losses.—The shock loss is attributed to a strong shock wave which eminates from the suction surface of the adjacent blade. Shock losses were obtained from a simple correlation which relates relative total pressure shock loss parameter to

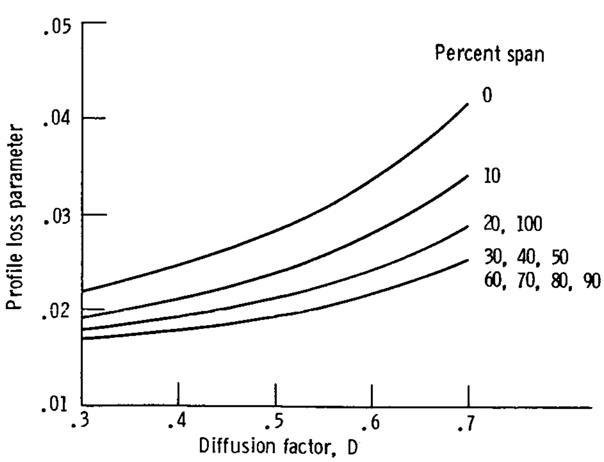

Figure 6.—Rotor profile losses. (See eqs. (B13) and (B21).)

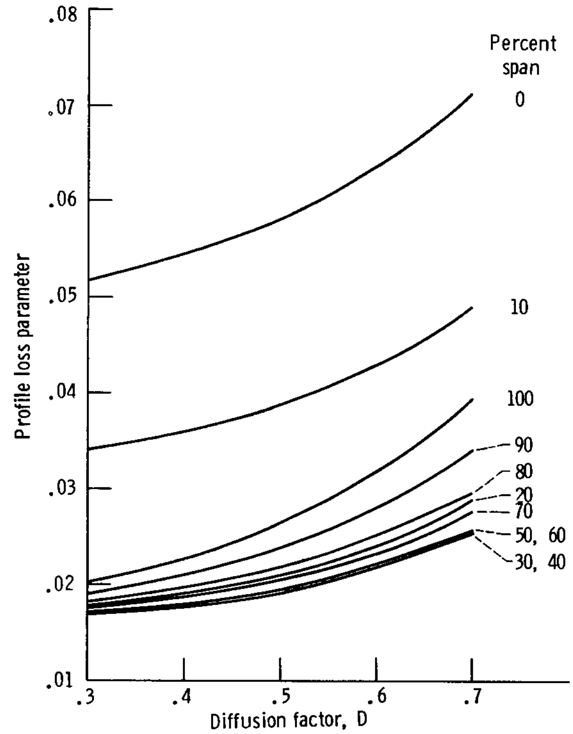

Figure 7.—Stator profile losses. (See eqs. (B13) and (B21).)

blade element relative inlet Mach number. With the data of references 2 to 11 as input, a single shock loss correlation was established for rotors and stators (fig. 8). This shock loss correlation predicts a shock loss parameter increase with increased blade inlet relative Mach number.

Blade Design

The basic goal of a blade design is to establish a blade shape that efficiently produces the required velocity diagrams at the blade inlet and outlet. The parameters which specify blade-element shape are (1) the incidence and deviation angles and (2) the blade camber and thickness distributions along the blade-element chord.

A circular arc blade shape is established in the compressor design computer code (ref. 1). The blade elements are defined

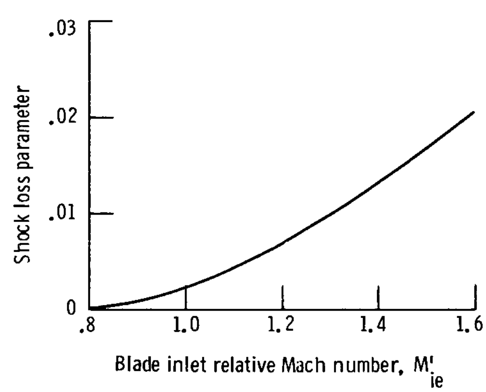

Figure 8.—Shock loss correlation.

on conical surfaces which pass through the blade streamline locations (fig. 9). Each blade element is composed of two segments. The blade centerline (mean camber line) and the two surfaces of each segment have a constant change of angle with path distance (fig. 10). A blade element is completely specified by the following: leading- and trailing-edge angles, K_{le} and K_{te}, and radii, R_{le} and R_{te}; maximum thickness T_m; location of maximum thickness C_m and transition point C_T; and the turning rate ratio C_1/C_2. When $C_1 \neq C_2$, the blade element shape is described as multiple circular arc (MCA). When $C_1 = C_2$ and the maximum thickness is at midchord, the blade shape is a double circular arc (DCA).

After the blade elements are defined, they are stacked about their centers of area along a prescribed stacking line. For manufacturing purposes fabrication coordinates are given on planes perpendicular to a radial line through the hub stacking point.

Incidence angle.—The incidence angles were selected to obtain minimum loss at design flow conditions. The incidence angles of similar blade rows (refs. 2 to 11) were examined for minimum loss values and applied to the current 74A design. For the three rotors of the inlet stage group, the design suction-surface incidence angles are all 0. For the stators the design suction-surface incidence angles were from $-1.0°$ to $-3.0°$. Generally, lower suction-surface incidence angles are used for blade elements with low inlet relative Mach numbers. For the IGV's design incidence angles are set at 0 relative to the blade mean camber line.

The selected rotor incidence angles were compared with those calculated by a method described in reference 13. This method, which is valid for free-stream Mach numbers above 1.0, requires that suction-surface incidence angle be set at a point that is one-half the distance to the first captured shock wave such that capture area ratio equals unity. This method was intended to control the shock wave pattern (fig. 11) and minimize shock loss. The selected design rotor incidence angles were within 1.0° of the calculated incidence angles (ref. 13), and all produce capture area ratios above unity and generally within 7 percent of unity.

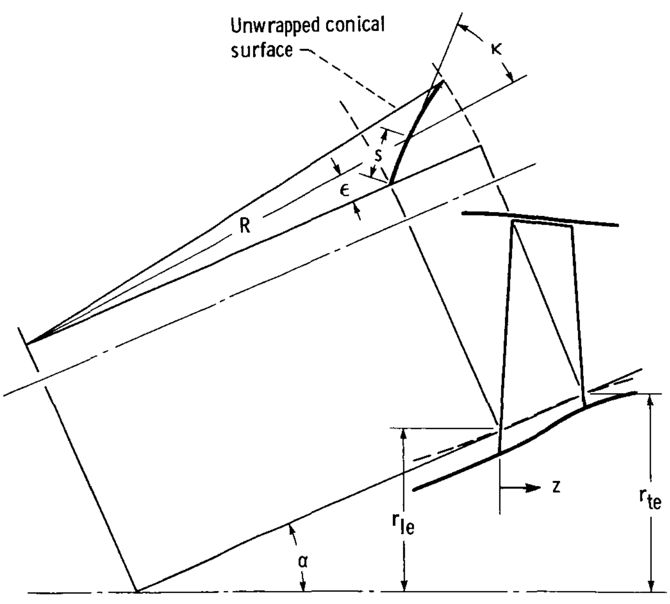

Figure 9.—Conical coordinate system for blade-element layout.

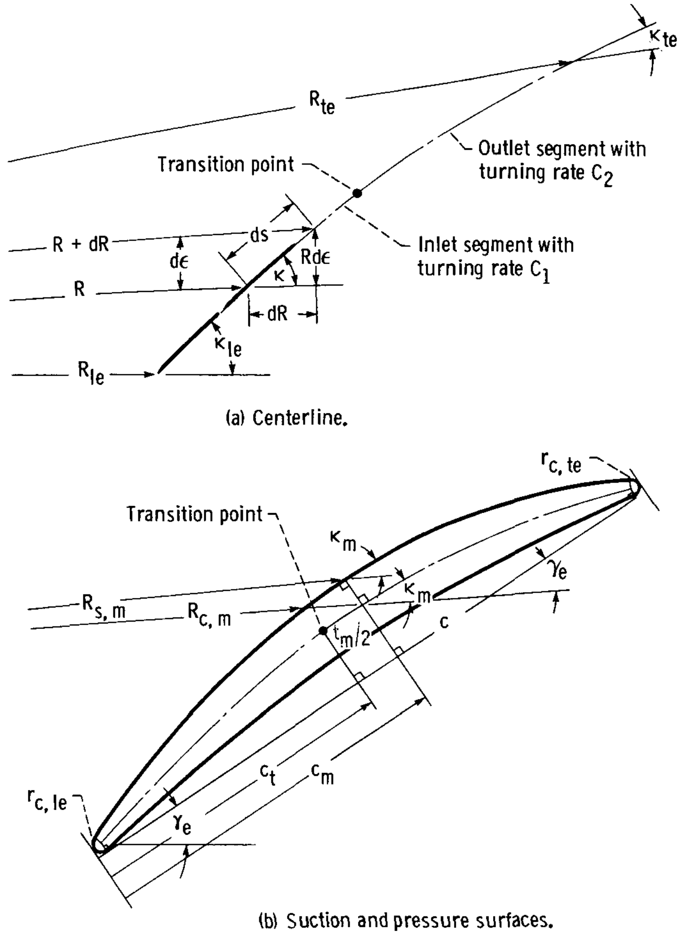

(a) Centerline.
(b) Suction and pressure surfaces.
Figure 10.—Blade-element layout parameters.

Deviation angle.—Rotor and stator design deviation angles are based on experimental deviation angles measured near the design operating conditions (refs. 2 to 11). For the IGV design deviation angles are 0. The selected design rotor and stator deviation angles are higher, especially at the tip and hub, than those obtained using Carter's rule. Figure 12 shows the rotor and stator deviation angle adjustment factors which were added to Carter's rule deviation angles to get the selected design deviation angles.

Blade shape.—Thin blades were selected for improved aerodynamic performance. Blade thicknesses are sufficient for acceptable manufacturing tolerance and structural integrity. All rotor and stator blades for compressor 74A are thickest at midchord and have small leading-edge wedge angles. Blades having low inlet relative Mach numbers (all stators and rotor 3), were of double circular arc (DCA) shape. Blades having supersonic inlet relative Mach numbers (the midspan to tip regions of rotors 1 and 2) were of multiple circular arc (MCA)

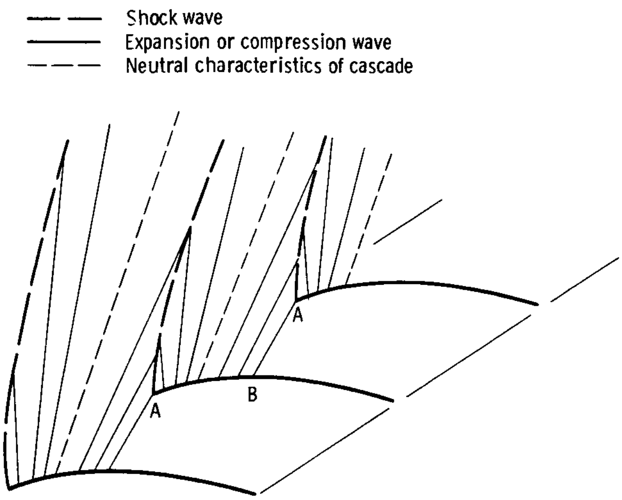

Figure 11.—Extended wave pattern ahead of supersonic cascade with curved entrance region AB.

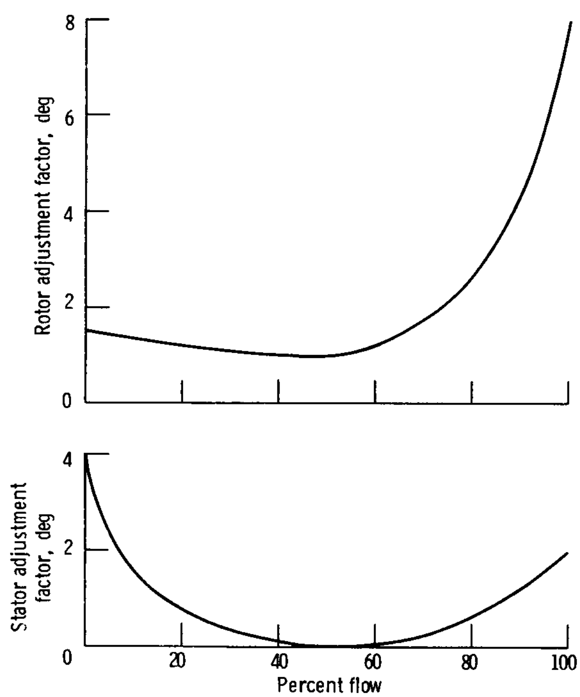

Figure 12.—Deviation adjustment factors added to Carter's rule.

shape. The MCA blade shape reduces suction surface turning and improves inlet shock wave pattern, resulting in less loss. The MCA blade shapes are specified by rotor blade-element inlet to outlet mean camber line turning ratios of less than 1.0. Design turning rate ratio and choke margin are plotted in figures 13 and 14. For rotor 1, which has the highest tip region inlet relative Mach number, the tip region turning rate ratio was reduced in an attempt to minimize the shock losses.

Aerodynamic Design Tables

The aerodynamic design tables provide a complete detailed numerical documentation of the aerodynamic design. They are computer generated from the compressor design program output. Tables II and III list design overall stage parameters for all five stages of compressor 74A. Tables IV and V list radial distributions of blade aerodynamic and geometric parameters for the inlet stage group (first three stages) of compressor 74A. Appendix C gives the definitions and units used in the design tables.

Mechanical Design

Blade stress and vibration information is presented for the inlet stage group. The rotor blades were made of titanium (TI-GAL-4V), and the stator blades of maraging steel (18 NI 200).

Blade Stress

Goodman diagrams are in figure 15. Factors of safety (yield strength divided by calculated combined maximum stress at design speed) are in table VI. For all rotor blades the combined stress was minimized by stacking the blade elements at

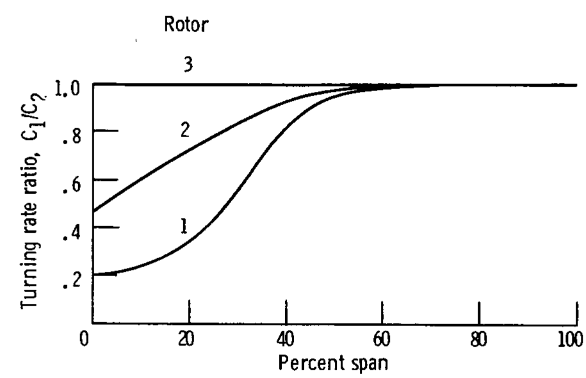

Figure 13.—Rotor blade element turning rate ratio.

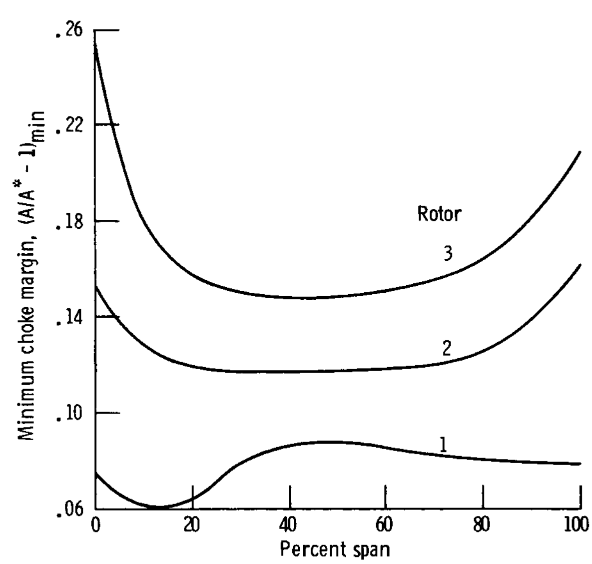

Figure 14.—Rotor blade element choke margin.

design speed to counterbalance the bending moments of steady-state aerodynamic forces and centrifugal force. Rotor 1 blades have the highest calculated maximum stress, which equals about half of the yield strength. The stator blades all have low maximum stresses of less than 10 percent of yield strength.

Blade Vibration

The Campbell diagrams of figure 16 show that the rotor blade resonance curves intersect the excitations per revolution lines at those rotational speeds which cause possible rotor blade vibration problems. For all the rotor blades the first bending resonance curve is above the two-excitations-per-revolution line. The first bending resonance curve intersects the four-excitations-per-revolution line at 50 percent speed for rotor 1 and at 90 percent speed for rotor 2. For rotor 3 first blending resonance is above four excitations per revolution.

Apparatus and Procedure

Compressor Test Facility

The multistage compressor test facility is described in detail in reference 14. A schematic diagram of the facility is shown in figure 17. Briefly, atmospheric air enters the test facility at an inlet located on the roof of the building and flows through the flow measuring orifice, through two inlet butterfly throttle valves, and into the plenum chamber upstream of the test compressor. The air then passes through the test compressor and into the collector and exits the collector either to the atmosphere or to an altitude exhaust system. Mass flow is controlled with a sleeve valve in the collector. For this series of tests, both inlet butterfly throttle valves were partially closed to maintain a constant compressor inlet pressure of 5.066 N/cm^2 and the air was exhausted through the altitude exhaust system.

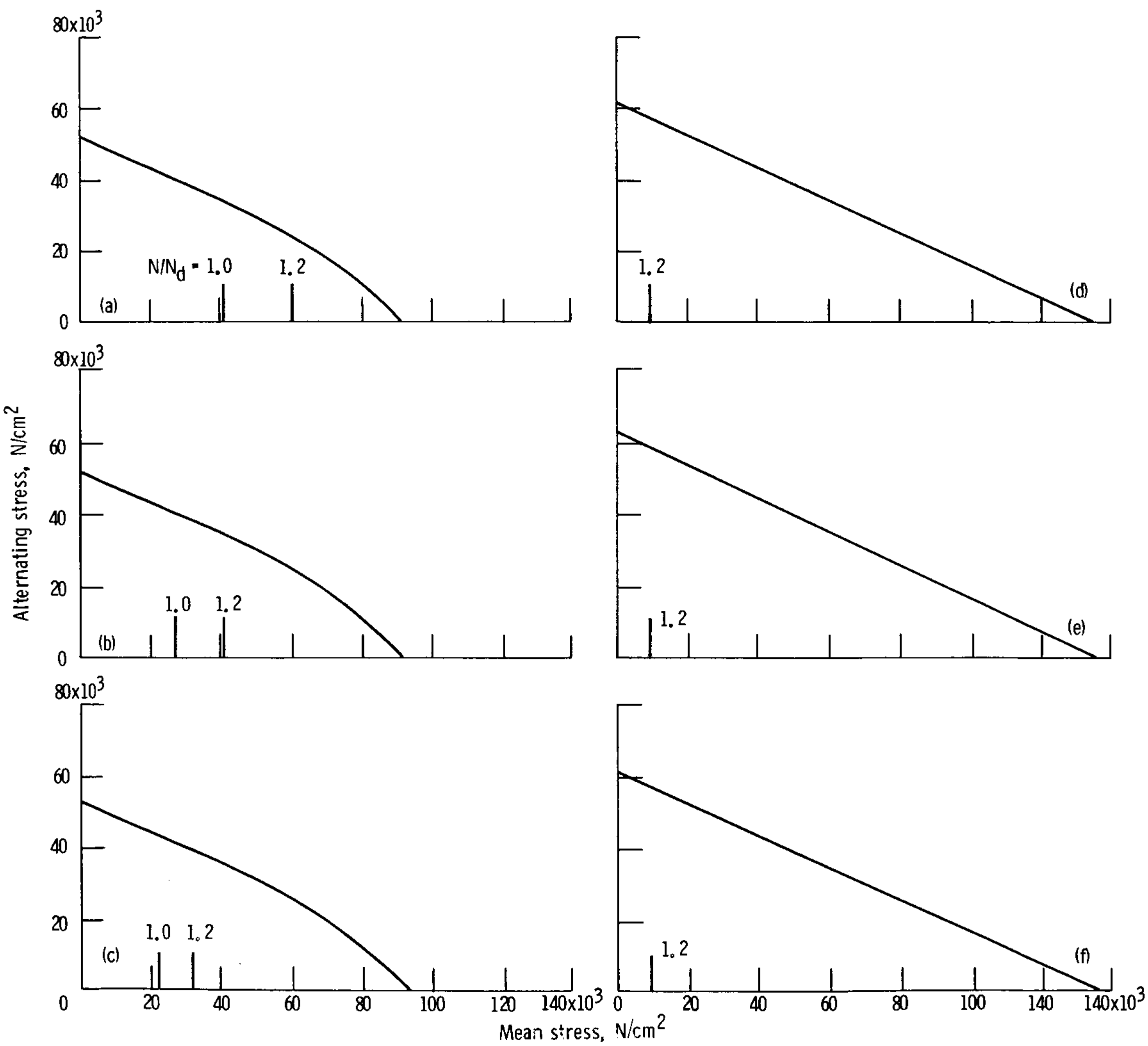

(a) Rotor 1.
(b) Rotor 2.
(c) Rotor 3.
(d) Stator 1.
(e) Stator 2.
(f) Stator 3.

Figure 15.—Goodman diagrams.

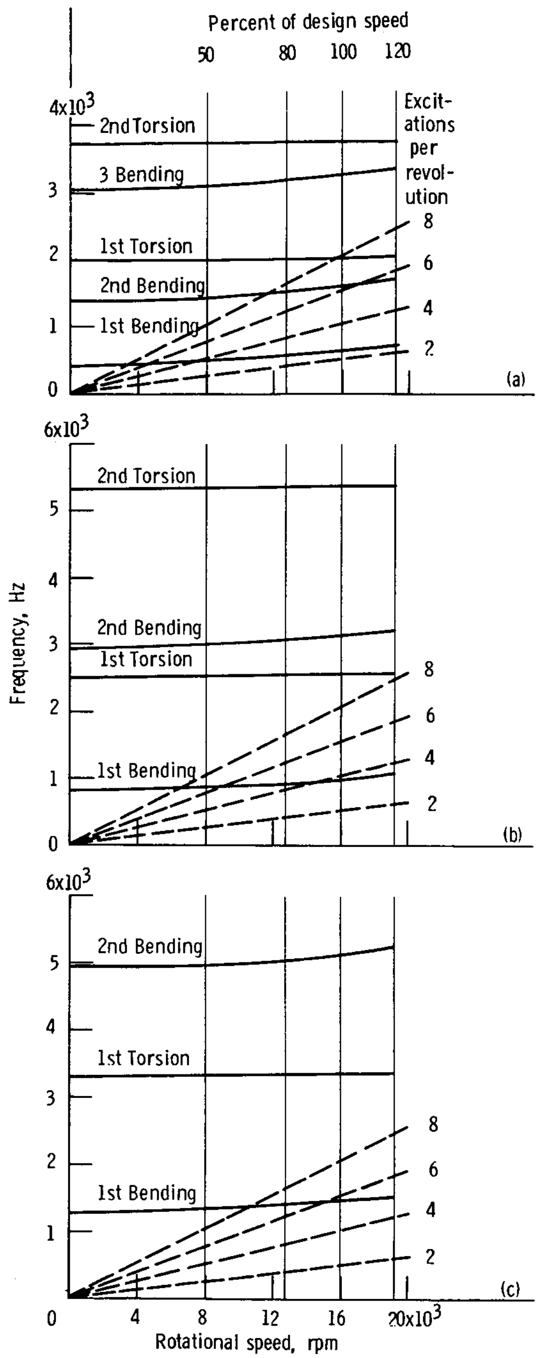

(a) Rotor 1. (b) Rotor 2. (c) Rotor 3.

Figure 16.—Campbell diagrams for rotors.

Instrumentation

Two iron-constantan thermocouples were located in the compressor inlet plenum for sensing compressor inlet total temperature. Compressor inlet total pressure was assumed equal to plenum static pressure, which was measured by four manifolded wall static taps located ~90° apart in the plenum tank. The compressor outlet conditions were determined from measurements obtained from four rakes located ~90° apart 6.8 cm downstream of the third-stage stator row. Each rake had five total-pressure–total-temperature elements located at 10, 30, 50, 70, and 90 percent span from the outer casing. The thermocouple material for the rakes was Chromel-constantan.

Static pressures at each rake element location were interpreted from a linear variation between the inner and outer wall static-pressure measurements. The compressor mass flow was determined with a standardized ASME thin-plate orifice. An electronic speed counter, with a magnetic pickup, was used to measure rotative speed (rpm). The estimated errors of the data, based on inherent accuracies of the instrumentation and recording system, are as follows:

Mass flow, kg/sec	±0.3
Temperature, K	±0.6
Inlet total pressure, N/cm^2	±0.1
Outlet total pressure, N/cm^2	±0.41
Outlet static pressure, N/cm^2	±0.41
Rotative speed, rpm	±30

Test Procedure

Data were recorded at 60, 70, 80, 85, 90, 95, and 100 percent of design speed. At each speed data were recorded over a range of flows from maximum flow to stall. The stall points were established by increasing the back pressure until stall occurred. Stall was indicated by a significant drop in outlet total pressure, an increase in audible noise level, and a large increase in rotor stress levels.

Data Reduction Procedure

The overall compressor performance is based on average conditions in the plenum tank and mass-averaged values of total pressure and total temperature at the compressor outlet. The rake temperatures were corrected for Mach number. All performance parameters were corrected to standard-day conditions based on plenum measurements.

Overall Performance Results

The overall performance of the inlet stage group of compressor 74A, for three IGV-stator setting angle schedules, are presented in figures 18 to 22.

Design IGV-Stator Setting Angles

The performance of the compressor at design IGV-stator settings is presented in figure 18. At design speed the compressor overflows and does not achieve its design efficiency. Significant deterioration occurred above 90 percent of design speed.

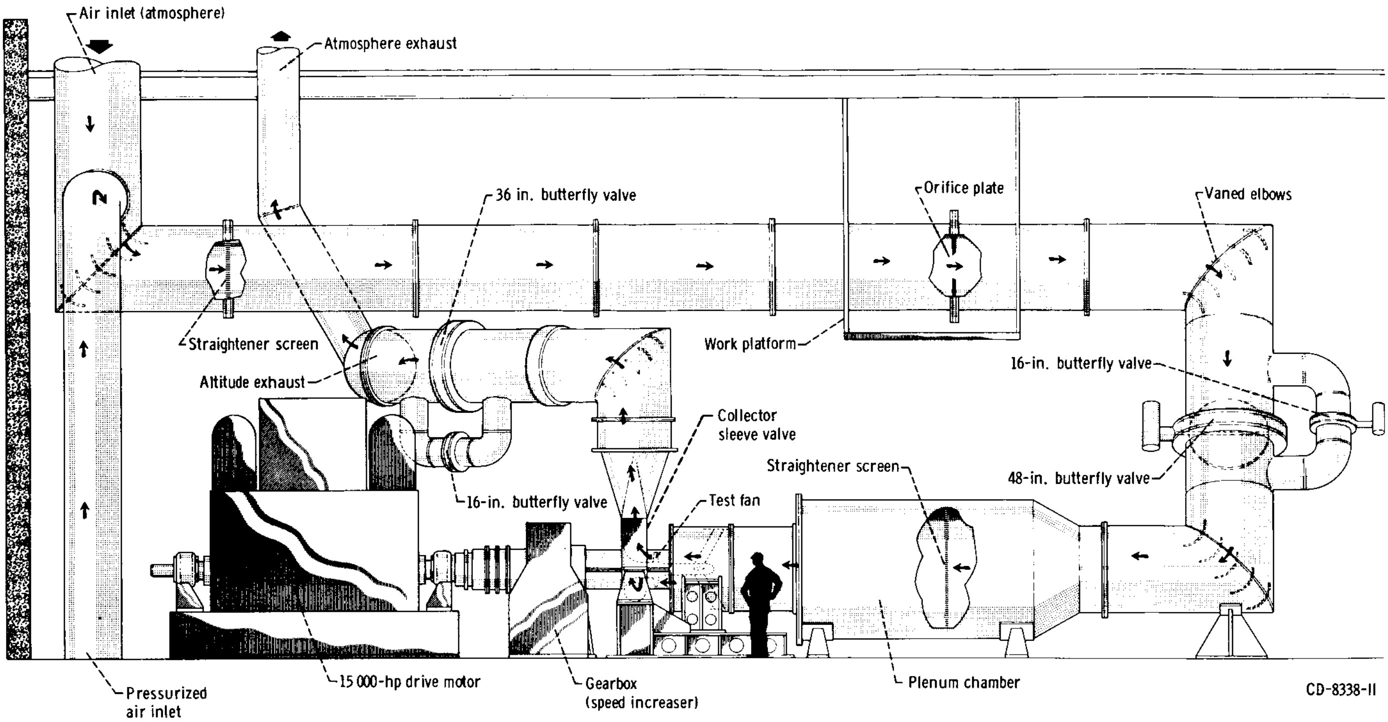

Figure 17.—Multistage compressor test facility.

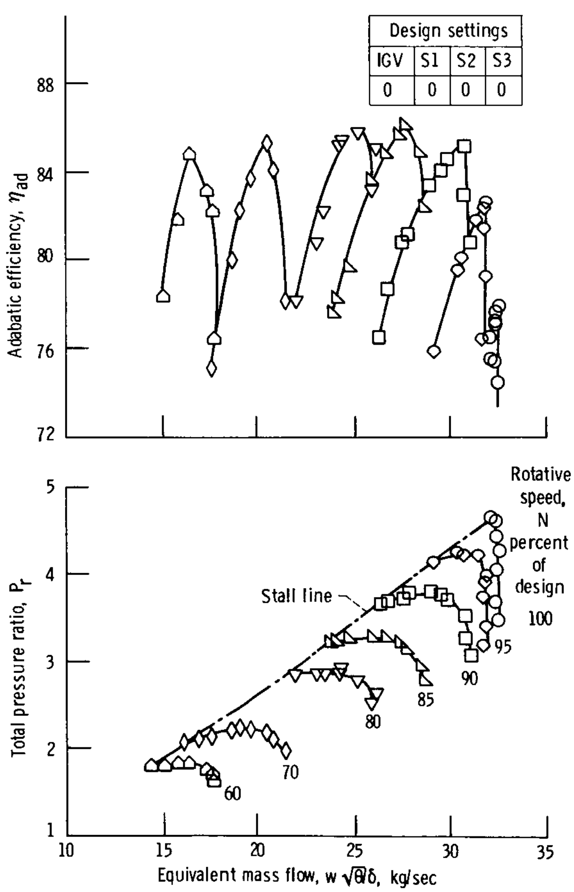

Figure 18.—Performance of first three stages of compressor 74A at design IGV-stator setting angles.

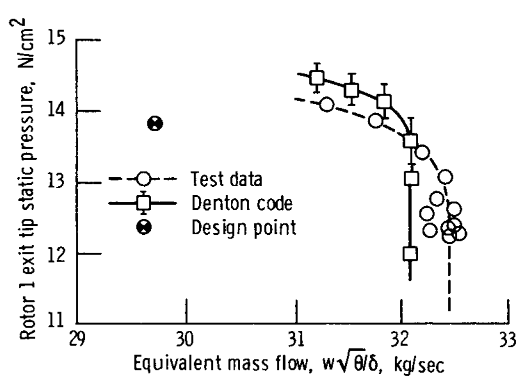

Figure 19.—Comparison of measured and computed rotor 1 exit tip static pressure versus mass flow.

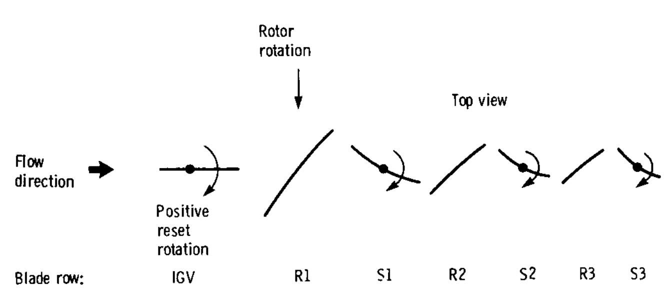

Figure 20.—Schematic of blade rows with positive direction of vane reset specified.

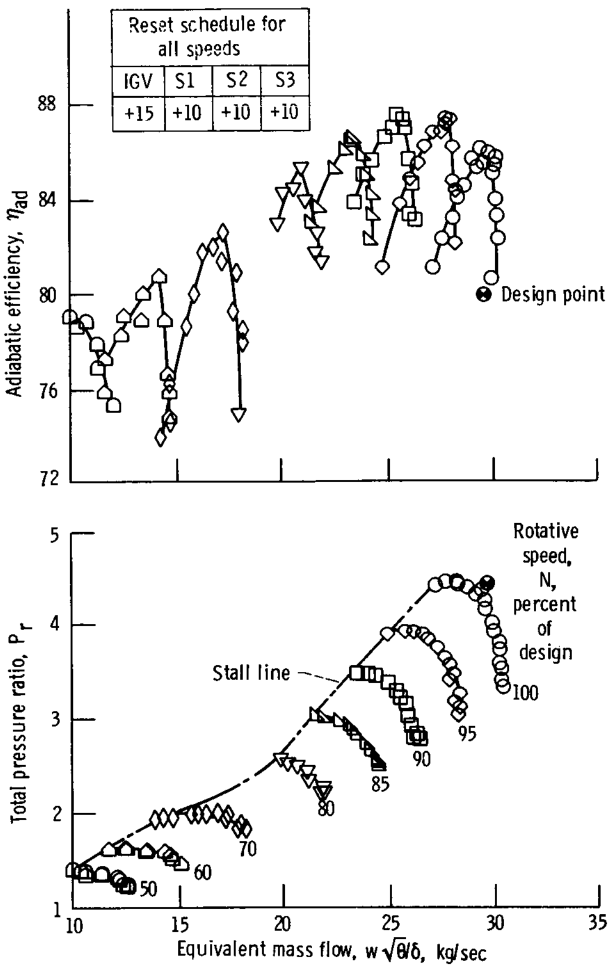

Figure 21.—Performance of first three stages of compressor 74A at optimized IGV-stator setting angles for maximum efficiency at design speed.

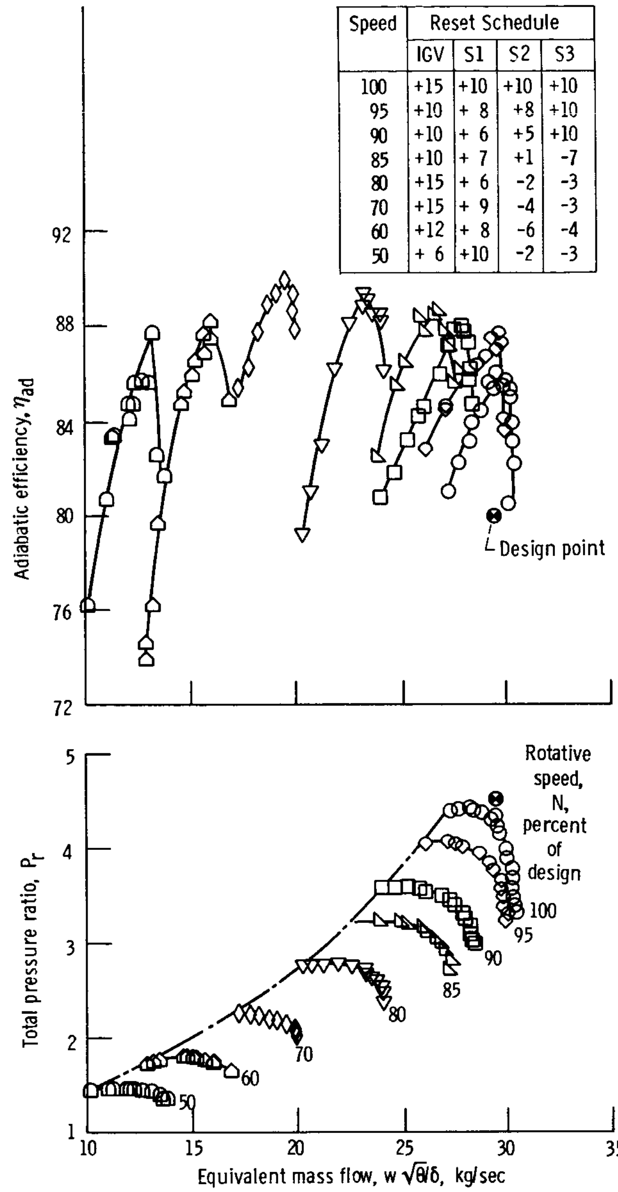

Figure 22.—Performance of first three stages of compressor 74A at optimized IGV-stator setting angles for maximum efficiency at each speed shown.

Because the large overflow (9.1 percent of design flow) at design speed was inconsistent with past experience in predicting choke margin for transonic rotors, a confirmation of the overflow was undertaken. The three-dimensional blade row analysis code developed by Denton (ref. 15) was applied to rotor 1. Previous experience with the Denton code on another transonic, low aspect ratio axial blade row had yielded excellent agreement between calculated and measured choke flow rate. Figure 19 shows measured and calculated rotor-exit tip static pressure versus flow. The calculation indicates that the first rotor did actually overflow by the amount indicated by the measurements.

Optimized IGV-Stator Setting Angles

A vane reset optimization computer program developed by Pratt & Whitney Aircraft under contract to the United States Air Force (ref. 16) was used to reset the vanes for optimum compressor adiabatic efficiency. The design speed peak adiabatic efficiency was obtained by resetting the IGV's +15° and each stator blade row +10° (fig. 20). Compressor performance for this reset schedule is presented in figure 21. At design speed the compressor operated at design flow and reduced total pressure ratio; and, adiabatic efficiency increased ~6 points to about 0.86. Between 85 and 100 percent of design speed, efficiency was improved, but below 85 percent of design speed, efficiency deteriorated rapidly.

The IGV-stator settings, optimized for maximum overall adiabatic efficiency, were next determined for each part speed. The reset schedules and the compressor performance are presented in figure 22 for each speed. Adiabatic efficiency exceeded 0.86 over entire performance map and peaked at ~0.90 at 70 percent design speed. Excellent stall margin was obtained at all speed lines.

Remarks

For the core inlet stage group (first three stages), the detailed blade-element design was dependent on shock and profile loss correlations and incidence and deviation angles based on single-stage data from similar blading. It is not known how a multistage environment affects a single-stage data application. Comparisons of blade-edge test data with the design parameters may reveal the suitability of single-stage data to multistage designs.

For multistage designs, especially those with highly loaded stages, a good design (which enables the compressor to perform as designed) is essential to good performance. Off-design operation of a stage forces the next stage into off-design operation. Highly loaded stage performance deteriorates rapidly at off-design operation. Stage matching techniques such as the use of stator reset can be used to improve the performance of a poorly designed compressor, but stage matching is not a substitute for good compressor design. In fact, a very good design would eliminate the need for stage matching.

This report suggests a building block approach to the design of advanced compressors whereby individual stage groups are designed and evaluated. The best matched inlet, middle, and exit stage groups would be selected for the complete compressor. This approach reduces design time and cost and permits the substitution of stage groups. For example the inlet stage group could be considered for both an axial flow and centrifugal flow configuration. However, the success of this approach requires that the individual stage groups match well in the environment of the complete compressor. To the extent that the matching of stage groups is similar to the matching of stages to form a stage group, a good design of each stage group appears essential to minimize matching problems. The difficulty of designing a good stage group from single-stage data, may be a preview to the difficulty of designing a complete compressor with good performance from stage groups.

Summary of Results

This report presented the design of the advanced axial flow core compressor 74A. The first three stages were fabricated and experimentally evaluated. Overall performance tests were conducted. The principal test results are

1. At design IGV-stator setting angles and speed, design pressure ratio was obtained at a flow higher than design flow and an adiabatic efficiency 2 percentage points less than design.
2. For IGV-stator setting angles optimized for maximum adiabatic efficiency, a peak adiabatic efficiency of 0.86 was obtained at design speed near design flow. At part speeds peak adiabatic efficiencies were 0.87 to 0.89 with reset IGV and stator blades.

Lewis Research Center
National Aeronautics and Space Administration
Cleveland, Ohio, February 1986

Appendix A

Symbols

A_{an}	annulus area at blade leading edge, m^2
A_f	frontal area at blade leading edge, m^2
A/A^*	critical area ratio
C	blade surface segment change of angle with path distance, cm^{-1}
c	blade chord, cm
C_p	specific heat at constant pressure, $m^2/(sec^2\ K)$
D	diffusion factor
i	incidence angle, deg
K	local blade angle with respect to meridional direction, deg
M	Mach number
N	rotative speed, rpm
P	total pressure, N/cm^2
p	static pressure, N/cm^2
R	radial coordinate on blade element layout cone, cm
r	radius, cm
s	path distance on blade element layout cone, cm
T	total temperature, K
t	blade element thickness, cm
U	wheel speed, m/sec
V	velocity, m/sec
w	mass flow, kg/sec
α	angle of streamline with respect to axial direction, deg
β	air angle, angle between air velocity and axial direction, deg
β_c^1	relative meridional air angle based on blade element core angle, deg
γ	ratio of specific heats
λ_e	blade chord angle, deg
δ	ratio of total pressure to standard pressure of 10.13 N/cm^2
$\delta°$	deviation angle, angle between exit air direction and tangent to blade mean camber line at trailing edge, deg
ϵ	angular coordinate on blade element layout cone, rad
η	efficiency
σ	solidity
θ	ratio of total temperature to standard temperature of 288.2 K
κ	blade angle relative to local conic ray (fig. 9)
τ	temperature rise coefficient
Φ	flow coefficient
ϕ	camber angle, deg
Ψ	head rise coefficient
$\bar{\omega}$	total loss coefficient
$\bar{\omega}_p$	profile loss coefficient
$\bar{\omega}_s$	shock loss coefficient

Subscripts:

ad	adiabatic
c	blade element centerline on cone
d	design
id	ideal
le	leading edge
m	meridional direction
mc	blade mean line
min	minimum
p	polytropic
r	ratio
ss	suction surface
t	tip
te	trailing edge
tot	total
tr	transition point
z	axial direction
θ	tangential direction
1	inlet blade segment
2	outlet blade segment

Superscript:

$'$	relative to blade

Appendix B

Equations

Equivalent mass flow—

$$\frac{w\sqrt{\theta}}{\delta} \tag{B1}$$

Equivalent speed—

$$\frac{N}{\sqrt{\theta}} \tag{B2}$$

Mass flow per unit annulus area—

$$\frac{w\sqrt{\theta}}{\delta A_{an}} \tag{B3}$$

Mass flow per unit frontal area—

$$\frac{w\sqrt{\theta}}{\delta A_f} \tag{B4}$$

Flow coefficient—

$$\Phi = \frac{V_z}{(U_t)_{le}} \tag{B5}$$

Head rise coefficient—

$$\Psi = C_p \frac{T_{le}}{U_t^2}\left[\left(\frac{P_{te}}{P_{le}}\right)^{(\gamma-1)/\gamma} - 1\right] \tag{B6}$$

Temperature rise coefficient—

$$\tau = \frac{C_p}{U_t^2}(T_{le} - T_{te}) \tag{B7}$$

Adiabatic efficiency—

$$\eta_{ad} = \frac{(P_{te}/P_{le})^{(\gamma-1)/\gamma} - 1}{(T_{te} - T_{le}) - 1} \tag{B8}$$

Polytropic efficiency—

$$\eta_p = \frac{\ln\,(P_{te} - P_{le})^{(\gamma-1)/\gamma}}{\ln\,(T_{te}/T_{le})} \tag{B9}$$

Total loss coefficient—

$$\bar{\omega} = \frac{(P'_{id})_{te} - P'_{te}}{P'_{le} - p_{le}} \tag{B10}$$

Profile loss coefficient—

$$\bar{\omega}_p = \bar{\omega} - \bar{\omega}_s \tag{B11}$$

Total loss parameter—

$$\frac{\bar{\omega}\cos\,(\beta'_m)_{te}}{2\sigma} \tag{B12}$$

Profile loss parameter—

$$\frac{\bar{\omega}_p\cos\,(\beta'_m)_{te}}{2\sigma} \tag{B13}$$

Suction-surface incidence angle—

$$i_{ss} = (\beta'_c)_{le} - (\kappa_{ss})_{le} \tag{B14}$$

Mean incidence angle—

$$i_{mc} = (\beta'_c)_{le} - (\kappa_{mc})_{le} \tag{B15}$$

Deviation angle—

$$\delta^\circ = (\beta'_c)_{te} - (\kappa_{mc})_{te} \tag{B16}$$

Front suction-surface camber—

$$\Phi_{f,ss} = (\kappa_{ss})_{le} - (\kappa_{ss})_{tr} \tag{B17}$$

Total camber—

$$\Phi_{tot} = (\kappa_{mc})_{le} - (\kappa_{mc})_{le} \tag{B18}$$

Turning rate ratio—

$$(C_1/C_2) \tag{B19}$$

Minimum choke margin—

$$(A/A^* - 1.0)_{min} \tag{B20}$$

Diffusion factor—

$$D = 1 - \frac{V'_{te}}{V'_{le}} + \frac{(rV_\theta)_{te} - (rV_\theta)_{le}}{(r_{te} + r_{le})\sigma(V'_{le})} \tag{B21}$$

Appendix C

Definitions and Units Used in Aerodynamic Design Tables

ABS	absolute
AERO CHORD	aerodynamic chord, cm
BETAM	meridional air angle, deg
CHOKE MARGIN	ratio of flow area greater than critical area to critical area
CONE ANGLE	angle between axial direction and conical surface representing blade element, deg
DELTA INC	difference between mean camber blade angle and suction-surface blade angle at leading edge, deg
DEV	deviation angle (defined by eq. (B16)), deg
D-FACT	diffusion factor (defined by eq. (B21))
EFF	adiabatic efficiency (defined by eq. (B8))
IN	inlet (leading edge of blade)
INCIDENCE	incidence angle (suction surface defined by eq. (B14)) and mean by eq. (B15)), deg
KIC	angle between blade-element mean camber line on conical surface at leading edge and meridional plane, deg
KOC	angle between blade-element mean camber line on conical surface at trailing edge and meridional plane, deg
KTC	angle between blade-element mean camber line on conical surface at transition point and meridional plane, deg
LOSS COEFF	loss coefficient (total defined by eq. (B10) and profile by eq. (B11))
LOSS PARAM	loss parameter (total defined by eq. (B12) and profile by eq. (B13))
MERID	meridional
MERID VEL R	meridional velocity ratio
OUT	outlet (trailing edge of blade)
PERCENT SPAN	percent of blade span from tip reference to rotor one outlet
PHISS	suction-surface camber ahead of assumed shock location, deg
PRESS	pressure, N/cm^2
PROF	profile
RADII	radius, cm
REL	relative to blade
RI	inlet radius (leading edge of blade), cm
RO	outlet radius (trailing edge of blade), cm
RP	radial position
RPM	equivalent rotative speed, rpm
SETTING ANGLE	angle between blade-element aerodynamic chord on conical surface and meridional plane, deg
SOLIDITY	ratio of aerodynamic chord to blade spacing
SPEED	speed, m/sec
SS	suction surface
STREAMLINE SLOPE	slope of streamline, deg
TANG	tangential
TEMP	temperature, K
TI	thickness of blade at leading edge, cm
TM	thickness of blade at maximum thickness, cm
TO	thickness of blade at trailing edge, cm
TOT	total
TOTAL CAMBER	difference between inlet and outlet blade-element angles on mean camber lines, deg (KIC-KOC)
TURNING RATIO	ratio of mean camber line curvatures upstream and downstream of transition point
VEL	velocity, m/sec
WT FLOW	equivalent weight flow, kg/sec
ZI	axial distance to blade leading edge, cm
ZMC	axial distance to blade maximum thickness point, cm
ZO	axial distance to blade trailing edge, cm
ZTC	axial distance to transition point, cm

References

1. Crouse, James E.; and Gorrell, William T.: Computer Program for Aerodynamic and Blading Design of Multistage Axial-Flow Compressors. NASA TP-1946, 1981.
2. Hager, Roy D.; Janetzke, David C.; and Reid, Lonnie: Performance of a 1380-Foot-per-Second-Tip-Speed Axial-Flow Compressor Rotor with a Blade Tip Solidity of 1.3. NASA TM X-2448, 1972.
3. Janetzke, David C.; Ball, Calvin L.; and Hager, Roy D.: Performance of a 1380-Foot-per-Second-Tip-Speed Axial-Flow Compressor Rotor with Blade Tip Solidity of 1.1. NASA TM X-2449, 1972.
4. Ball, Calvin L; Janetzke, David C.; and Reid, Lonnie: Performance of a 1380-Foot-per-Second-Tip-Speed Axial-Flow Compressor Rotor with Blade Tip Solidity of 1.5. NASA TM X-2379, 1972.
5. Reid, Lonnie; and Kovich, George: Overall and Blade Element Performance of a Transonic Compressor Stage with Multiple-Circular-Arc Blades at Tip Speed of 419 Meters per Second. NASA TM X-2731, 1973.
6. Kovich, George; Moore, Royce D.; and Urasek, Donald C.: Performance of Transonic Fan Stage with Weight Flow per Unit Annulus Area of 198 Kilograms per Second per Square Meter (40.6 (lb/sec)/ft^2). NASA TM X-2905, 1973.
7. Moore, Royce D.; and Reid, Lonnie: Performance of a Single-Stage Axial-Flow Transonic Compressor Stage with a Blade Tip Solidity of 1.7. NASA TM X-2658, 1972.
8. Urasek, Donald C.; Moore, Royce D.; and Osborn, Walter M.: Performance of a Single Stage Transonic Compressor with a Blade Tip Solidity of 1.3. NASA TM X-2645, 1972.
9. Moore, Royce D.; Urasek, Donald C.; and Kovich, George: Performance of Transonic Fan Stage with Weight Flow Per Unit Annulus Area of 178 Kilograms per Second per Square Meter (36.5/lb/sec)/(ft^2)). NASA TM X-2904, 1973.
10. Osborn, Walter M.; Urasek, Donald C.; and Moore, Royce D.: Performance of a Single-Stage Transonic Compressor with a Blade Tip Solidity of 1.5 and Comparison with 1.3 and 1.7-Solidity Stages. NASA TM X-2926, 1972.
11. Urasek, Donald C.; Kovich, George; and Moore, Royce D.: Performance of Transonic Fan Stage with Weight Flow Per Unit Annulus Area of 208 Kilograms per Second per Square Meter (42.6 (lb/sec)/ft^2). NASA TM X-2903, 1973.
12. Lieblein, Seymour; Schwenk, Francis C.; and Broderick, Robert L.: Diffusion Factor for Estimating Losses and Limiting Blade Loadings in Axial-Flow-Compressor Blade Elements. NACA RM-E53 DO1, 1953.
13. Messenger, H.E.; and Kennedy, E.E.: Two Stage Fan. 1: Aerodynamic and Mechanical Design. (PWA-4148, Pratt & Whitney Aircraft; NASA Contract NAS3-13494) NASA CR-120859, 1972.
14. Cunnan, Walter S.; Stevens, William; and Urasek, Donald C.: Design and Performance of a 427-Meter-per-Second-Tip-Speed Two-Stage Fan Having a 2.40 Pressure Ratio. NASA TP-1314, 1978.
15. Denton, J.D.: An Improved Time Marching Method for Turbomachinery Flow Calculations. J. Eng. Power, vol. 105, no. 3, July 1983, pp. 514-524.
16. Garberoglio, J.E.; Song, J.O.; and Boudreaux, W.L.: Optimization of Compressor Vane and Bleed Settings—User's Manual. AFWAL-TR-82-2078, Air Force Wright Aeronautical Lab, 1981. (AD-A119379.)

TABLE I.—BLADE ROW PARAMETERS

Blade row	Aspect ratio	Tip solidity	Number of blades
IGV	2.22	1.00	26
Rotor 1	1.45	1.35	28
Stator 1	1.53	1.42	34
Rotor 2	1.17	1.25	32
Stator 2	1.43	1.28	46
Rotor 3	1.04	1.21	39
Stator 3	1.19	1.23	54
Rotor 4	1.01	1.14	49
Stator 4	1.15	1.13	64
Rotor 5	1.02	1.09	62
Stator 5	1.11	1.08	74

TABLE II.—DESIGN OVERALL PERFORMANCE PARAMETERS FOR CORE COMPRESSOR 74A

Parameters	First three stages	Compressor 74A
Total pressure ratio	4.474	9.271
Total temperature ratio	1.663	2.095
Adiabatic efficiency	0.799	0.797
Polytropic efficiency	0.836	0.848
Mass flow per unit annulus area	193.173	193.173
Mass flow	29.710	29.710
Equivalent rotative speed, rpm	16 042.3	16 042.3
Tip speed, m/sec	430.29	430.291

TABLE III.—DESIGN OVERALL STAGE PERFORMANCE PARAMETERS

Parameter	Inlet guide vane	Stage 1	Stage 2	Stage 3	Stage 4	Stage 5
Rotor total pressure ratio	0.980	1.792	1.691	1.613	1.506	1.416
Stage total pressure ratio	0.980	1.743	1.654	1.581	1.483	1.399
Rotor total temperature ratio	1.000	1.209	1.181	1.159	1.133	1.110
Stage total temperature ratio	1.000	1.209	1.181	1.159	1.133	1.110
Rotor adiabatic efficiency	0	0.867	0.890	0.903	0.909	0.911
Stage adiabatic efficiency	0	0.823	0.849	0.863	0.873	0.877
Rotor polytropic efficiency	0	0.877	0.897	0.909	0.914	0.915
Stage polytropic efficiency	0	0.836	0.859	0.872	0.880	0.883
Rotor head rise coefficient	0	0.283	0.327	0.366	0.376	0.368
Stage head rise coefficient	0	0.269	0.312	0.350	0.361	0.355
Flow coefficient	0	0.464	0.477	0.484	0.500	0.512
Compressor inlet equivalent values						
Mass flow per unit frontal area	143.896	144.153	154.041	161.706	168.937	173.677
Mass flow per unit annulus area	172.954	189.310	276.435	385.163	528.411	691.489
Mass flow	29.710	29.710	29.710	29.710	29.710	29.710
Rotative speed, rpm	16 042.300	16 042.300	16 042.300	16 042.300	16 042.300	16 042.300
Tip speed	430.675	430.291	416.252	406.267	397.477	392.015
Stage inlet equivalent values						
Mass flow per unit frontal area	143.896	147.095	99.144	68.381	48.640	35.876
Mass flow per unit annulus area	172.954	193.173	177.919	162.876	152.140	142.838
Mass flow	29.710	30.317	19.122	12.564	8.554	6.137
Rotative speed, rpm	16 042.300	16 042.300	14 590.673	13 427.144	12 469.871	11 716.563
Tip speed	430.675	430.291	378.586	340.039	308.963	286.310

TABLE IV.—DESIGN-BLADE ELEMENT PARAMETERS

(a) Inlet guide wave

RP	RADII IN	RADII OUT	ABS BETAM IN	ABS BETAM OUT	REL BETAM IN	REL BETAM OUT	TOTAL TEMP IN	TOTAL TEMP RATIO	TOTAL PRESS IN	TOTAL PRESS RATIO
TIP	25.636	25.712	.0	.0	.0	.0	288.2	1.000	10.14	.980
1	25.065	25.147	.0	.0	.0	.0	288.2	1.000	10.14	.980
2	24.411	24.520	.0	.0	.0	.0	288.2	1.000	10.14	.980
3	23.082	23.259	.0	.0	.0	.0	288.2	1.000	10.14	.980
4	21.713	21.979	.0	.0	.0	.0	288.2	1.000	10.14	.980
5	20.308	20.683	.0	.0	.0	.0	288.2	1.000	10.14	.980
6	18.857	19.367	.0	.0	.0	.0	288.2	1.000	10.14	.980
7	17.347	18.018	.0	.0	.0	.0	288.2	1.000	10.14	.980
8	15.764	16.623	.0	.0	.0	.0	288.2	1.000	10.14	.980
9	14.082	15.171	.0	.0	.0	.0	288.2	1.000	10.14	.980
10	12.265	13.641	.0	.0	.0	.0	288.2	1.000	10.14	.980
11	11.295	12.840	.0	.0	.0	.0	288.2	1.000	10.14	.980
HUB	10.508	12.139	.0	.0	.0	.0	288.2	1.000	10.14	.980

RP	ABS VEL IN	ABS VEL OUT	REL VEL IN	REL VEL OUT	MERID VEL IN	MERID VEL OUT	TANG VEL IN	TANG VEL OUT	WHEEL SPEED IN	WHEEL SPEED OUT
TIP	172.7	185.9	172.7	185.9	172.7	185.9	.0	.0	.0	.0
1	172.3	186.5	172.3	186.5	172.3	186.5	.0	.0	.0	.0
2	171.9	187.2	171.9	187.2	171.9	187.2	.0	.0	.0	.0
3	171.0	189.3	171.0	189.3	171.0	189.3	.0	.0	.0	.0
4	170.1	191.1	170.1	191.1	170.1	191.1	.0	.0	.0	.0
5	169.0	192.2	169.0	192.2	169.0	192.2	.0	.0	.0	.0
6	167.5	192.5	167.5	192.5	167.5	192.5	.0	.0	.0	.0
7	165.6	191.8	165.6	191.8	165.6	191.8	.0	.0	.0	.0
8	162.9	189.9	162.9	189.9	162.9	189.9	.0	.0	.0	.0
9	159.4	186.6	159.4	186.6	159.4	186.6	.0	.0	.0	.0
10	154.8	181.3	154.8	181.3	154.8	181.3	.0	.0	.0	.0
11	152.1	177.6	152.1	177.6	152.1	177.6	.0	.0	.0	.0
HUB	149.9	174.5	149.9	174.5	149.9	174.5	.0	.0	.0	.0

RP	ABS MACH NO IN	ABS MACH NO OUT	REL MACH NO IN	REL MACH NO OUT	MERID MACH NO IN	MERID MACH NO OUT	STREAMLINE SLOPE IN	STREAMLINE SLOPE OUT	MERID VEL R	PEAK SS MACH NO
TIP	.521	.563	.521	.563	.521	.563	.15	.49	1.076	.521
1	.520	.565	.520	.565	.520	.565	.50	.31	1.082	.520
2	.518	.568	.518	.568	.518	.568	.89	.23	1.089	.518
3	.516	.574	.516	.574	.516	.574	1.58	.68	1.107	.516
4	.513	.580	.513	.580	.513	.580	2.30	1.60	1.123	.513
5	.509	.584	.509	.584	.509	.584	3.11	2.91	1.138	.509
6	.505	.585	.505	.585	.505	.585	4.05	4.53	1.149	.505
7	.498	.582	.498	.582	.498	.582	5.15	6.46	1.158	.498
8	.490	.576	.490	.576	.490	.576	6.47	8.73	1.165	.490
9	.479	.565	.479	.565	.479	.565	8.07	11.43	1.170	.479
10	.465	.548	.465	.548	.465	.548	9.99	14.87	1.171	.465
11	.456	.537	.456	.537	.456	.537	11.08	17.01	1.167	.456
HUB	.449	.527	.449	.527	.449	.527	11.96	18.89	1.164	.449

RP	PERCENT SPAN	INCIDENCE MEAN	INCIDENCE SS	DEV	D-FACT	EFF	LOSS COEFF TOT	LOSS COEFF PROF	LOSS PARAM TOT	LOSS PARAM PROF
TIP	.00	.0	-11.7	.0	-.076	.000	.118	.118	.060	.060
1	5.00	.0	-11.7	.0	-.082	.000	.119	.119	.059	.059
2	10.00	.0	-11.7	.0	-.089	.000	.119	.119	.057	.057
3	20.00	.0	-11.7	.0	-.107	.000	.121	.120	.055	.055
4	30.00	.0	-11.7	.0	-.123	.000	.122	.122	.052	.052
5	40.00	.0	-11.6	.0	-.138	.000	.123	.123	.049	.049
6	50.00	.0	-11.6	.0	-.149	.000	.125	.125	.047	.047
7	60.00	.0	-11.6	.0	-.158	.000	.128	.128	.044	.044
8	70.00	.0	-11.5	.0	-.165	.000	.132	.132	.042	.042
9	80.00	.0	-11.4	.0	-.170	.000	.138	.138	.039	.039
10	90.00	.0	-11.3	.0	-.171	.000	.145	.145	.036	.036
11	95.00	.0	-11.2	.0	-.167	.000	.150	.150	.035	.035
HUB	100.00	.0	-11.1	.0	-.164	.000	.155	.155	.033	.033

TABLE IV.—Continued.

(b) Rotor 1

RP	RADII IN	RADII OUT	ABS BETAM IN	ABS BETAM OUT	REL BETAM IN	REL BETAM OUT	TOTAL TEMP IN	TOTAL TEMP RATIO	TOTAL PRESS IN	TOTAL PRESS RATIO
TIP	25.613	24.973	.0	42.2	67.1	55.7	288.2	1.232	9.93	1.792
1	25.057	24.468	.0	42.6	65.9	55.0	288.2	1.228	9.93	1.792
2	24.444	23.963	.0	42.9	64.7	54.2	288.2	1.224	9.93	1.792
3	23.229	22.952	.0	43.4	62.7	52.0	288.2	1.218	9.93	1.792
4	22.008	21.941	.0	43.8	60.9	49.3	288.2	1.212	9.93	1.792
5	20.776	20.931	.0	44.6	59.3	45.9	288.2	1.208	9.93	1.792
6	19.520	19.920	.0	45.4	57.7	41.8	288.2	1.205	9.93	1.792
7	18.229	18.909	.0	46.2	56.1	37.0	288.2	1.202	9.93	1.792
8	16.889	17.899	.0	47.1	54.5	31.2	288.2	1.200	9.93	1.792
9	15.483	16.888	.0	48.0	52.7	24.4	288.2	1.197	9.93	1.792
10	13.993	15.877	.0	49.2	50.7	16.6	288.2	1.195	9.93	1.792
11	13.211	15.372	.0	49.9	49.5	12.2	288.2	1.195	9.93	1.792
HUB	12.509	14.867	.0	50.5	48.4	7.6	288.2	1.194	9.93	1.792

RP	ABS VEL IN	ABS VEL OUT	REL VEL IN	REL VEL OUT	MERID VEL IN	MERID VEL OUT	TANG VEL IN	TANG VEL OUT	WHEEL SPEED IN	WHEEL SPEED OUT
TIP	181.9	238.6	467.2	313.6	181.9	176.7	.0	160.4	430.3	419.5
1	188.4	237.7	441.2	305.3	188.4	174.9	.0	160.9	420.9	411.0
2	194.5	237.2	454.4	297.1	194.5	173.8	.0	161.5	410.6	402.6
3	201.7	238.4	439.3	281.6	201.7	173.4	.0	163.7	390.2	385.6
4	205.9	240.9	423.2	266.2	205.9	173.7	.0	166.9	369.7	368.6
5	207.6	244.7	406.1	250.5	207.6	174.3	.0	171.7	349.0	351.6
6	207.5	249.7	388.1	235.1	207.5	175.2	.0	177.9	327.9	334.6
7	205.8	255.6	368.9	221.2	205.8	176.8	.0	184.6	306.2	317.7
8	202.6	262.7	348.7	209.1	202.6	178.9	.0	192.4	283.7	300.7
9	198.2	270.9	327.0	199.0	198.2	181.2	.0	201.4	260.1	283.7
10	192.6	280.4	303.9	191.3	192.6	183.3	.0	212.2	235.1	266.7
11	189.4	285.9	291.7	188.5	189.4	184.2	.0	218.6	221.9	258.2
HUB	186.7	291.4	281.1	187.0	186.7	185.3	.0	224.9	210.2	249.8

RP	ABS MACH NO IN	ABS MACH NO OUT	REL MACH NO IN	REL MACH NO OUT	MERID MACH NO IN	MERID MACH NO OUT	STREAMLINE SLOPE IN	STREAMLINE SLOPE OUT	MERID VEL R	PEAK SS MACH NO
TIP	.550	.659	1.414	.865	.550	.488	-6.75	-7.92	.971	1.677
1	.571	.657	1.399	.844	.571	.483	-5.61	-6.24	.929	1.663
2	.591	.657	1.381	.822	.591	.481	-4.42	-4.67	.894	1.649
3	.615	.662	1.339	.782	.615	.481	-2.32	-2.07	.859	1.622
4	.628	.671	1.292	.742	.628	.484	-.22	.35	.844	1.624
5	.634	.684	1.240	.700	.634	.487	1.91	2.63	.839	1.613
6	.634	.700	1.185	.659	.634	.491	4.10	4.86	.844	1.595
7	.628	.720	1.126	.623	.628	.498	6.44	7.13	.859	1.571
8	.618	.743	1.063	.591	.618	.506	9.00	9.48	.883	1.550
9	.603	.769	.995	.565	.603	.515	11.91	11.96	.914	1.530
10	.585	.801	.923	.546	.585	.523	15.43	14.56	.952	1.414
11	.575	.818	.885	.540	.575	.527	17.58	15.90	.973	1.347
HUB	.566	.837	.852	.537	.566	.532	19.50	17.24	.993	1.289

RP	PERCENT SPAN	INCIDENCE MEAN	INCIDENCE SS	DEV	D-FACT	EFF	LOSS COEFF TOT	LOSS COEFF PROF	LOSS PARAM TOT	LOSS PARAM PROF
TIP	.00	2.8	-.2	6.3	.456	.781	.190	.067	.040	.014
1	5.00	3.1	-.1	6.3	.464	.795	.179	.062	.037	.013
2	10.00	3.4	-.1	6.3	.472	.808	.168	.058	.035	.012
3	20.00	3.9	-.0	6.2	.486	.833	.151	.053	.032	.011
4	30.00	4.4	-.0	6.0	.499	.854	.135	.045	.029	.010
5	40.00	4.9	.0	6.1	.514	.870	.126	.046	.027	.010
6	50.00	5.3	-.0	6.6	.529	.883	.120	.052	.026	.011
7	60.00	5.8	-.0	7.6	.540	.896	.114	.059	.025	.013
8	70.00	6.1	-.0	9.2	.546	.908	.108	.066	.024	.014
9	80.00	6.3	-.0	11.4	.544	.920	.104	.073	.022	.016
10	90.00	6.4	.0	14.8	.531	.928	.104	.093	.022	.019
11	95.00	6.3	.1	17.2	.519	.931	.107	.103	.021	.021
HUB	100.00	6.2	.1	19.5	.504	.934	.109	.108	.021	.021

TABLE IV.—Continued.

(c) Stator 1

RP	RADII IN	OUT	ABS BETAM IN	OUT	REL BETAM IN	OUT	TOTAL TEMP IN	RATIO	TOTAL PRESS IN	RATIO
TIP	24.846	24.826	41.4	.0	41.4	.0	355.1	1.000	17.80	.949
1	24.362	24.336	41.6	.0	41.6	.0	353.9	1.000	17.80	.958
2	23.876	23.879	41.8	.0	41.8	.0	352.8	1.000	17.80	.966
3	22.903	23.010	42.1	.0	42.1	.0	350.9	1.000	17.80	.978
4	21.930	22.164	42.5	.0	42.5	.0	349.3	1.000	17.80	.980
5	20.958	21.327	43.1	.0	43.1	.0	348.2	1.000	17.80	.979
6	19.987	20.495	43.9	.0	43.9	.0	347.4	1.000	17.80	.978
7	19.013	19.663	44.6	.0	44.6	.0	346.5	1.000	17.80	.976
8	18.039	18.830	45.5	.0	45.5	.0	345.7	1.000	17.80	.973
9	17.067	17.997	46.4	.0	46.4	.0	345.0	1.000	17.80	.969
10	16.104	17.167	47.5	.0	47.5	.0	344.5	1.000	17.80	.963
11	15.629	16.752	48.1	.0	48.1	.0	344.3	1.000	17.80	.959
HUB	15.156	16.279	48.7	.0	48.7	.0	344.2	1.000	17.80	.954

RP	ABS VEL IN	OUT	REL VEL IN	OUT	MERID VEL IN	OUT	TANG VEL IN	OUT	WHEEL SPEED IN	OUT
TIP	244.0	167.1	244.0	167.1	183.2	167.1	161.2	.0	.0	.0
1	243.4	176.2	243.4	176.2	182.0	176.2	161.6	.0	.0	.0
2	243.2	183.7	243.2	183.7	181.2	183.7	162.1	.0	.0	.0
3	244.6	193.2	244.6	193.2	181.5	193.2	164.0	.0	.0	.0
4	247.2	196.7	247.2	196.7	182.3	196.7	166.9	.0	.0	.0
5	251.0	197.5	251.0	197.5	183.3	197.5	171.5	.0	.0	.0
6	255.8	197.5	255.8	197.5	184.5	197.5	177.3	.0	.0	.0
7	261.4	196.8	261.4	196.8	186.0	196.8	183.6	.0	.0	.0
8	267.8	195.3	267.8	195.3	187.9	195.3	190.9	.0	.0	.0
9	275.2	192.9	275.2	192.9	189.8	192.9	199.3	.0	.0	.0
10	283.7	189.0	283.7	189.0	191.7	189.0	209.2	.0	.0	.0
11	288.6	186.3	288.6	186.3	192.6	186.3	215.0	.0	.0	.0
HUB	293.5	183.4	293.5	183.4	193.6	183.4	220.6	.0	.0	.0

RP	ABS MACH NO IN	OUT	REL MACH NO IN	OUT	MERID MACH NO IN	OUT	STREAMLINE SLOPE IN	OUT	MERID VEL R	PEAK SS MACH NO
TIP	.675	.451	.675	.451	.507	.451	-3.01	-5.19	.912	1.136
1	.674	.478	.674	.478	.504	.478	-2.25	-3.91	.968	1.130
2	.675	.500	.675	.500	.503	.500	-1.48	-2.80	1.014	1.128
3	.681	.529	.681	.529	.505	.529	.07	-1.04	1.065	1.140
4	.691	.540	.691	.540	.509	.540	1.76	.66	1.079	1.162
5	.704	.543	.704	.543	.514	.543	3.52	2.37	1.077	1.195
6	.719	.544	.719	.544	.519	.544	5.39	4.12	1.071	1.236
7	.738	.543	.738	.543	.525	.543	7.38	5.94	1.058	1.282
8	.759	.539	.759	.539	.532	.539	9.50	7.85	1.040	1.334
9	.783	.533	.783	.533	.540	.533	11.77	9.86	1.016	1.396
10	.811	.522	.811	.522	.548	.522	14.15	11.97	.986	1.469
11	.827	.514	.827	.514	.552	.514	15.38	13.06	.968	1.511
HUB	.844	.506	.844	.506	.556	.506	16.59	14.30	.948	1.556

RP	PERCENT SPAN	INCIDENCE MEAN	SS	DEV	D-FACT	EFF	LOSS COEFF TOT	PROF	LOSS PARAM TOT	PROF
TIP	.00	4.4	-3.0	13.9	.548	.000	.195	.195	.069	.069
1	5.00	4.3	-2.9	12.1	.509	.000	.160	.160	.056	.056
2	10.00	4.2	-2.8	10.9	.478	.000	.129	.129	.045	.045
3	20.00	4.1	-2.6	10.2	.443	.000	.081	.081	.028	.028
4	30.00	3.9	-2.3	10.1	.436	.000	.073	.073	.025	.025
5	40.00	3.7	-2.1	10.2	.445	.000	.075	.075	.026	.026
6	50.00	3.5	-1.9	10.5	.460	.000	.077	.077	.026	.026
7	60.00	3.3	-1.7	10.9	.479	.000	.080	.080	.027	.027
8	70.00	3.1	-1.4	11.5	.502	.000	.084	.084	.028	.028
9	80.00	2.9	-1.2	12.4	.530	.000	.092	.090	.030	.029
10	90.00	2.7	-1.0	13.4	.564	.000	.105	.097	.034	.031
11	95.00	2.6	-.9	14.0	.584	.000	.114	.101	.036	.032
HUB	100.00	2.5	-.7	14.7	.605	.000	.124	.105	.039	.033

TABLE IV.—Continued.

(d) Rotor 2

RP	RADII IN	RADII OUT	ABS BETAM IN	ABS BETAM OUT	REL BETAM IN	REL BETAM OUT	TOTAL TEMP IN	TOTAL TEMP RATIO	TOTAL PRESS IN	TOTAL PRESS RATIO
TIP	24.778	24.300	.0	46.3	66.8	53.3	355.2	1.203	16.88	1.735
1	24.307	23.868	.0	45.2	65.6	52.5	353.9	1.196	17.05	1.718
2	23.867	23.504	.0	44.4	64.4	51.8	352.8	1.190	17.19	1.703
3	23.025	22.800	.0	43.4	62.6	50.2	350.9	1.182	17.41	1.682
4	22.201	22.110	.0	43.6	61.4	48.3	349.3	1.179	17.44	1.679
5	21.390	21.433	.0	44.3	60.4	46.1	348.2	1.178	17.42	1.681
6	20.581	20.765	.0	45.0	59.4	43.6	347.4	1.178	17.40	1.683
7	19.773	20.107	.0	45.7	58.5	40.8	346.5	1.177	17.36	1.686
8	18.966	19.462	.0	46.5	57.7	37.6	345.7	1.177	17.32	1.691
9	18.161	18.835	.0	47.4	56.9	34.1	345.0	1.177	17.25	1.698
10	17.355	18.230	.0	48.7	56.3	30.1	344.5	1.178	17.14	1.709
11	16.950	17.937	.0	49.5	56.1	27.8	344.3	1.180	17.06	1.716
HUB	16.487	17.556	.0	50.5	55.8	24.7	344.1	1.182	16.97	1.725

RP	ABS VEL IN	ABS VEL OUT	REL VEL IN	REL VEL OUT	MERID VEL IN	MERID VEL OUT	TANG VEL IN	TANG VEL OUT	WHEEL SPEED IN	WHEEL SPEED OUT
TIP	178.2	247.4	452.8	286.3	178.2	171.1	.0	178.7	416.3	408.2
1	185.6	246.3	448.5	285.1	185.6	173.6	.0	174.8	408.3	401.0
2	191.8	245.7	444.5	283.8	191.8	175.5	.0	171.9	400.9	394.9
3	200.5	245.6	435.7	278.7	200.5	178.4	.0	168.8	386.8	383.0
4	203.7	247.0	425.0	269.1	203.7	178.9	.0	170.4	373.0	371.4
5	204.3	249.5	413.4	257.6	204.3	178.5	.0	174.3	359.3	360.1
6	204.2	252.6	401.5	246.6	204.2	178.6	.0	178.7	345.8	348.8
7	203.2	256.3	389.4	236.2	203.2	178.9	.0	183.5	332.2	337.8
8	201.5	260.4	377.0	226.3	201.5	179.3	.0	188.8	318.6	327.0
9	198.7	264.9	364.1	216.6	198.7	179.3	.0	195.0	305.1	316.4
10	194.4	270.1	350.4	206.3	194.4	178.4	.0	202.8	291.6	306.3
11	191.5	273.2	343.2	200.7	191.5	177.5	.0	207.6	284.8	301.3
HUB	188.3	277.2	334.9	194.2	188.3	176.4	.0	213.8	277.0	294.9

RP	ABS MACH NO IN	ABS MACH NO OUT	REL MACH NO IN	REL MACH NO OUT	MERID MACH NO IN	MERID MACH NO OUT	STREAMLINE SLOPE IN	STREAMLINE SLOPE OUT	MERID VEL R	PEAK SS MACH NO
TIP	.483	.620	1.227	.717	.483	.429	-7.67	-5.58	.960	1.692
1	.505	.620	1.220	.718	.505	.437	-6.07	-4.46	.935	1.675
2	.524	.621	1.213	.717	.524	.444	-4.66	-3.53	.915	1.662
3	.550	.625	1.196	.709	.550	.454	-2.38	-1.81	.890	1.641
4	.561	.631	1.170	.688	.561	.457	-.35	-.19	.878	1.630
5	.564	.640	1.140	.660	.564	.458	1.56	1.40	.874	1.625
6	.564	.649	1.109	.634	.564	.459	3.44	2.96	.875	1.620
7	.562	.660	1.077	.609	.562	.461	5.34	4.48	.880	1.620
8	.557	.673	1.043	.585	.557	.463	7.28	5.96	.890	1.625
9	.550	.686	1.008	.561	.550	.465	9.31	7.40	.902	1.638
10	.538	.701	.969	.536	.538	.463	11.44	8.72	.918	1.621
11	.529	.710	.949	.522	.529	.461	12.57	9.30	.927	1.610
HUB	.520	.721	.925	.505	.520	.459	13.86	10.06	.936	1.596

RP	PERCENT SPAN	INCIDENCE MEAN	INCIDENCE SS	DEV	D-FACT	EFF	LOSS COEFF TOT	LOSS COEFF PROF	LOSS PARAM TOT	LOSS PARAM PROF
TIP	.00	3.3	-.0	6.8	.526	.835	.153	.057	.037	.014
1	5.00	3.6	-.1	6.5	.517	.851	.136	.045	.033	.011
2	10.00	3.9	-.0	6.3	.511	.861	.126	.039	.030	.009
3	20.00	4.4	-.0	6.0	.506	.875	.111	.032	.027	.008
4	30.00	5.0	-.0	5.9	.513	.887	.103	.030	.025	.007
5	40.00	5.5	.0	6.1	.526	.893	.101	.033	.025	.008
6	50.00	6.0	.0	6.5	.538	.900	.098	.036	.024	.009
7	60.00	6.5	.0	7.3	.549	.906	.096	.038	.024	.009
8	70.00	6.9	.1	8.4	.560	.912	.094	.040	.024	.010
9	80.00	7.4	.1	10.0	.571	.918	.092	.040	.023	.010
10	90.00	7.8	.1	13.1	.584	.923	.093	.049	.023	.012
11	95.00	7.9	.2	15.3	.592	.924	.095	.056	.024	.014
HUB	100.00	8.2	.2	17.9	.603	.925	.098	.064	.025	.016

TABLE IV.—Continued.

(e) Stator 2

RP	RADII IN	RADII OUT	ABS BETAM IN	ABS BETAM OUT	REL BETAM IN	REL BETAM OUT	TOTAL TEMP IN	TOTAL TEMP RATIO	TOTAL PRESS IN	TOTAL PRESS RATIO
TIP	24.206	24.193	45.1	.0	45.1	.0	427.4	1.001	29.28	.957
1	23.798	23.785	43.8	.0	43.8	.0	423.2	1.000	29.28	.966
2	23.451	23.459	42.9	.0	42.9	.0	420.0	1.000	29.28	.972
3	22.778	22.837	41.8	.0	41.8	.0	414.9	1.000	29.28	.983
4	22.121	22.236	42.0	.0	42.0	.0	412.0	1.000	29.28	.983
5	21.472	21.648	42.7	.0	42.7	.0	410.3	1.000	29.28	.982
6	20.831	21.074	43.5	.0	43.5	.0	409.1	1.000	29.28	.981
7	20.196	20.512	44.3	.0	44.3	.0	407.9	1.000	29.28	.980
8	19.573	19.964	45.2	.0	45.2	.0	406.8	1.000	29.28	.978
9	18.962	19.430	46.2	.0	46.2	.0	406.1	1.000	29.28	.975
10	18.367	18.917	47.7	.0	47.7	.0	406.0	1.000	29.28	.972
11	18.076	18.671	48.7	.0	48.7	.0	406.3	1.000	29.28	.970
HUB	17.706	18.308	49.9	.0	49.9	.0	406.6	1.000	29.28	.967

RP	ABS VEL IN	ABS VEL OUT	REL VEL IN	REL VEL OUT	MERID VEL IN	MERID VEL OUT	TANG VEL IN	TANG VEL OUT	WHEEL SPEED IN	WHEEL SPEED OUT
TIP	253.4	176.2	253.4	176.2	179.0	176.2	179.4	.0	.0	.0
1	253.3	181.3	253.3	181.3	182.8	181.3	175.3	.0	.0	.0
2	253.2	185.2	253.2	185.2	185.6	185.2	172.3	.0	.0	.0
3	253.3	191.4	253.3	191.4	188.7	191.4	169.0	.0	.0	.0
4	254.5	193.0	254.5	193.0	189.1	193.0	170.3	.0	.0	.0
5	256.4	193.5	256.4	193.5	188.3	193.5	174.0	.0	.0	.0
6	258.8	194.0	258.8	194.0	187.7	194.0	178.2	.0	.0	.0
7	261.6	193.9	261.6	193.9	187.3	193.9	182.7	.0	.0	.0
8	264.9	193.4	264.9	193.4	186.8	193.4	187.8	.0	.0	.0
9	268.4	192.5	268.4	192.5	185.8	192.5	193.7	.0	.0	.0
10	272.3	191.3	272.3	191.3	183.4	191.3	201.3	.0	.0	.0
11	274.4	190.8	274.4	190.8	181.3	190.8	206.0	.0	.0	.0
HUB	277.3	189.9	277.3	189.9	178.8	189.9	212.0	.0	.0	.0

RP	ABS MACH NO IN	ABS MACH NO OUT	REL MACH NO IN	REL MACH NO OUT	MERID MACH NO IN	MERID MACH NO OUT	STREAMLINE SLOPE IN	STREAMLINE SLOPE OUT	MERID VEL R	PEAK SS MACH NO
TIP	.636	.433	.636	.433	.450	.433	-2.37	1.33	.984	1.170
1	.639	.449	.639	.449	.461	.449	-1.70	.68	.992	1.141
2	.642	.461	.642	.461	.471	.461	-1.14	.33	.998	1.121
3	.646	.480	.646	.480	.482	.480	-.05	.46	1.014	1.103
4	.652	.486	.652	.486	.485	.486	1.10	1.06	1.021	1.110
5	.659	.488	.659	.488	.484	.488	2.29	1.95	1.028	1.130
6	.667	.490	.667	.490	.484	.490	3.52	3.00	1.034	1.153
7	.676	.491	.676	.491	.484	.491	4.80	4.14	1.036	1.178
8	.686	.490	.686	.490	.484	.490	6.10	5.33	1.036	1.207
9	.697	.488	.697	.488	.482	.488	7.41	6.52	1.036	1.242
10	.708	.485	.708	.485	.477	.485	8.68	7.68	1.043	1.286
11	.714	.484	.714	.484	.471	.484	9.28	8.24	1.052	1.314
HUB	.721	.481	.721	.481	.465	.481	10.04	9.07	1.063	1.352

RP	PERCENT SPAN	INCIDENCE MEAN	INCIDENCE SS	DEV	D-FACT	EFF	LOSS COEFF TOT	LOSS COEFF PROF	LOSS PARAM TOT	LOSS PARAM PROF
TIP	.00	5.1	-3.0	15.0	.583	.000	.180	.180	.071	.071
1	5.00	5.0	-3.0	12.6	.553	.000	.143	.143	.056	.056
2	10.00	4.8	-2.9	11.2	.531	.000	.114	.114	.044	.044
3	20.00	4.6	-2.8	10.2	.497	.000	.070	.070	.027	.027
4	30.00	4.3	-2.7	9.8	.490	.000	.070	.070	.026	.026
5	40.00	4.0	-2.5	9.8	.493	.000	.072	.072	.026	.026
6	50.00	3.7	-2.4	9.9	.497	.000	.074	.074	.027	.027
7	60.00	3.4	-2.3	10.2	.503	.000	.077	.077	.027	.027
8	70.00	3.1	-2.2	10.7	.513	.000	.082	.082	.028	.028
9	80.00	2.8	-2.1	11.4	.524	.000	.089	.089	.030	.030
10	90.00	2.5	-2.0	12.6	.539	.000	.098	.098	.033	.033
11	95.00	2.3	-2.0	13.3	.547	.000	.105	.105	.034	.034
HUB	100.00	2.1	-1.9	14.3	.558	.000	.113	.113	.037	.037

TABLE IV.—Continued.

(f) Rotor 3

RP	RADII IN	RADII OUT	ABS BETAM IN	ABS BETAM OUT	REL BETAM IN	REL BETAM OUT	TOTAL TEMP IN	TOTAL TEMP RATIO	TOTAL PRESS IN	TOTAL PRESS RATIO
TIP	24.183	23.769	.0	46.8	68.4	49.6	427.5	1.174	28.03	1.648
1	23.772	23.410	.0	45.9	66.4	49.3	423.2	1.168	28.28	1.633
2	23.441	23.147	.0	45.2	64.9	49.1	420.0	1.164	28.48	1.622
3	22.826	22.640	.0	44.2	63.0	48.2	414.9	1.159	28.78	1.605
4	22.240	22.146	.0	44.5	61.8	46.9	412.0	1.158	28.77	1.605
5	21.671	21.666	.0	45.2	61.0	45.4	410.3	1.158	28.75	1.607
6	21.116	21.194	.0	45.8	60.3	43.7	409.1	1.158	28.73	1.608
7	20.573	20.735	.0	46.4	59.6	41.8	407.9	1.158	28.69	1.610
8	20.042	20.290	.0	46.9	59.1	39.7	406.8	1.158	28.64	1.613
9	19.525	19.861	.0	47.6	58.6	37.6	406.1	1.158	28.57	1.617
10	19.024	19.454	.0	48.4	58.3	35.1	406.0	1.159	28.47	1.623
11	18.780	19.261	.0	48.9	58.1	33.8	406.3	1.160	28.40	1.626
HUB	18.420	18.951	.0	49.6	58.0	31.6	406.6	1.161	28.31	1.631

RP	ABS VEL IN	ABS VEL OUT	REL VEL IN	REL VEL OUT	MERID VEL IN	MERID VEL OUT	TANG VEL IN	TANG VEL OUT	WHEEL SPEED IN	WHEEL SPEED OUT
TIP	160.8	260.6	436.9	275.2	160.8	178.6	.0	189.9	406.3	399.3
1	174.5	257.4	435.8	275.0	174.5	179.2	.0	184.7	399.4	393.3
2	184.2	255.4	434.8	274.7	184.2	179.9	.0	181.3	393.8	388.9
3	195.7	253.6	430.5	272.9	195.7	181.8	.0	176.8	383.5	380.3
4	200.1	254.1	423.8	265.3	200.1	181.2	.0	178.2	373.6	372.0
5	201.8	255.6	416.3	256.4	201.8	180.1	.0	181.4	364.1	364.0
6	202.7	257.6	408.6	248.2	202.7	179.5	.0	184.7	354.7	356.1
7	202.6	259.9	400.6	240.5	202.6	179.3	.0	188.1	345.6	348.3
8	201.8	262.5	392.6	233.1	201.8	179.3	.0	191.8	336.7	340.9
9	200.3	265.5	384.3	226.0	200.3	179.1	.0	195.9	328.0	333.7
10	197.7	269.0	375.8	218.6	197.7	178.7	.0	201.0	319.6	326.8
11	196.0	271.1	371.4	214.6	196.0	178.4	.0	204.1	315.5	323.6
HUB	193.7	274.4	365.1	208.8	193.7	177.8	.0	209.0	309.4	318.4

RP	ABS MACH NO IN	ABS MACH NO OUT	REL MACH NO IN	REL MACH NO OUT	MERID MACH NO IN	MERID MACH NO OUT	STREAMLINE SLOPE IN	STREAMLINE SLOPE OUT	MERID VEL R	PEAK SS MACH NO
TIP	.395	.602	1.073	.636	.395	.412	-3.78	-7.37	1.110	1.801
1	.432	.599	1.079	.640	.432	.417	-3.23	-5.74	1.027	1.747
2	.459	.597	1.082	.642	.459	.421	-2.74	-4.62	.977	1.710
3	.492	.598	1.082	.644	.492	.429	-1.67	-2.82	.929	1.665
4	.505	.602	1.070	.629	.505	.429	-.48	-1.27	.906	1.648
5	.511	.607	1.053	.609	.511	.428	.79	.14	.892	1.643
6	.514	.613	1.036	.591	.514	.427	2.10	1.45	.886	1.644
7	.515	.620	1.017	.574	.515	.428	3.42	2.66	.885	1.652
8	.513	.628	.998	.558	.513	.429	4.72	3.79	.888	1.664
9	.509	.636	.978	.541	.509	.429	5.99	4.83	.895	1.656
10	.503	.645	.955	.524	.503	.428	7.19	5.73	.904	1.657
11	.498	.650	.944	.515	.498	.428	7.75	6.11	.910	1.663
HUB	.492	.658	.926	.500	.492	.426	8.58	6.73	.918	1.670

RP	PERCENT SPAN	INCIDENCE MEAN	INCIDENCE SS	DEV	D-FACT	EFF	LOSS COEFF TOT	LOSS COEFF PROF	LOSS PARAM TOT	LOSS PARAM PROF
TIP	.00	3.5	-.2	6.6	.550	.869	.128	.028	.035	.008
1	5.00	3.9	-.1	6.5	.542	.885	.109	.022	.029	.006
2	10.00	4.3	-.1	6.3	.536	.891	.101	.023	.027	.006
3	20.00	4.9	-.0	6.1	.528	.900	.091	.023	.024	.006
4	30.00	5.4	-.0	6.1	.536	.906	.086	.024	.023	.006
5	40.00	6.0	.0	6.3	.549	.908	.087	.028	.023	.007
6	50.00	6.5	.0	6.7	.560	.911	.086	.029	.023	.008
7	60.00	6.9	.0	7.3	.569	.914	.086	.030	.023	.008
8	70.00	7.4	.0	8.2	.579	.917	.085	.029	.023	.008
9	80.00	7.8	.0	9.6	.588	.920	.084	.033	.023	.009
10	90.00	8.2	.0	12.3	.599	.922	.085	.036	.023	.010
11	95.00	8.4	.0	14.3	.606	.923	.087	.039	.024	.011
HUB	100.00	8.7	.0	17.2	.616	.922	.090	.043	.025	.012

TABLE IV.—Concluded.

(g) Stator 3

RP	RADII IN	RADII OUT	ABS BETAM IN	ABS BETAM OUT	REL BETAM IN	REL BETAM OUT	TOTAL TEMP IN	TOTAL TEMP RATIO	TOTAL PRESS IN	TOTAL PRESS RATIO
TIP	23.680	23.660	45.9	.0	45.9	.0	502.1	1.001	46.19	.961
1	23.337	23.323	44.6	.0	44.6	.0	494.3	1.000	46.19	.970
2	23.086	23.086	43.7	.0	43.7	.0	489.0	1.000	46.19	.976
3	22.607	22.639	42.6	.0	42.6	.0	480.8	1.000	46.19	.984
4	22.137	22.210	42.9	.0	42.9	.0	477.0	1.000	46.19	.984
5	21.679	21.793	43.6	.0	43.6	.0	475.1	1.000	46.19	.983
6	21.226	21.388	44.3	.0	44.3	.0	473.6	1.000	46.19	.983
7	20.784	20.993	45.0	.0	45.0	.0	472.2	1.000	46.19	.982
8	20.352	20.611	45.7	.0	45.7	.0	471.0	1.000	46.19	.980
9	19.935	20.246	46.5	.0	46.5	.0	470.3	1.000	46.19	.979
10	19.535	19.898	47.5	.0	47.5	.0	470.5	1.000	46.19	.976
11	19.340	19.732	48.2	.0	48.2	.0	471.1	1.000	46.19	.975
HUB	19.040	19.441	49.2	.0	49.2	.0	472.0	1.000	46.19	.972

RP	ABS VEL IN	ABS VEL OUT	REL VEL IN	REL VEL OUT	MERID VEL IN	MERID VEL OUT	TANG VEL IN	TANG VEL OUT	WHEEL SPEED IN	WHEEL SPEED OUT
TIP	265.1	182.3	265.1	182.3	184.3	182.3	190.5	.0	.0	.0
1	264.0	187.2	264.0	187.2	188.0	187.2	185.3	.0	.0	.0
2	263.2	190.5	263.2	190.5	190.4	190.5	181.8	.0	.0	.0
3	261.7	195.2	261.7	195.2	192.7	195.2	177.1	.0	.0	.0
4	262.0	195.9	262.0	195.9	191.9	195.9	178.3	.0	.0	.0
5	262.8	195.8	262.8	195.8	190.3	195.8	181.3	.0	.0	.0
6	264.0	195.8	264.0	195.8	189.0	195.8	184.4	.0	.0	.0
7	265.5	195.5	265.5	195.5	187.8	195.5	187.7	.0	.0	.0
8	267.2	194.8	267.2	194.8	186.7	194.8	191.2	.0	.0	.0
9	269.2	193.9	269.2	193.9	185.3	193.9	195.2	.0	.0	.0
10	271.4	192.7	271.4	192.7	183.2	192.7	200.2	.0	.0	.0
11	272.6	192.1	272.6	192.1	181.6	192.1	203.3	.0	.0	.0
HUB	274.6	191.1	274.6	191.1	179.4	191.1	208.0	.0	.0	.0

RP	ABS MACH NO IN	ABS MACH NO OUT	REL MACH NO IN	REL MACH NO OUT	MERID MACH NO IN	MERID MACH NO OUT	STREAMLINE SLOPE IN	STREAMLINE SLOPE OUT	MERID VEL R	PEAK SS MACH NO
TIP	.614	.414	.614	.414	.427	.414	-2.34	1.52	.989	1.159
1	.616	.429	.616	.429	.439	.429	-1.83	.94	.996	1.124
2	.617	.439	.617	.439	.447	.439	-1.44	.66	1.001	1.102
3	.619	.454	.619	.454	.456	.454	-.57	.73	1.013	1.077
4	.623	.458	.623	.458	.456	.458	.34	1.17	1.021	1.081
5	.626	.459	.626	.459	.453	.459	1.30	1.83	1.029	1.093
6	.630	.459	.630	.459	.451	.459	2.27	2.63	1.036	1.107
7	.635	.459	.635	.459	.449	.459	3.24	3.49	1.041	1.122
8	.640	.458	.640	.458	.447	.458	4.18	4.39	1.044	1.139
9	.646	.456	.646	.456	.445	.456	5.07	5.28	1.046	1.159
10	.652	.453	.652	.453	.440	.453	5.85	6.16	1.052	1.185
11	.654	.452	.654	.452	.436	.452	6.19	6.58	1.058	1.201
HUB	.659	.449	.659	.449	.430	.449	6.72	7.33	1.066	1.226

RP	PERCENT SPAN	INCIDENCE MEAN	INCIDENCE SS	DEV	D-FACT	EFF	LOSS COEFF TOT	LOSS COEFF PROF	LOSS PARAM TOT	LOSS PARAM PROF
TIP	.00	5.8	-3.0	15.7	.606	.000	.176	.176	.072	.072
1	5.00	5.6	-3.0	13.1	.574	.000	.134	.134	.054	.054
2	10.00	5.4	-3.0	11.6	.552	.000	.107	.107	.043	.043
3	20.00	5.0	-3.0	10.7	.518	.000	.069	.069	.027	.027
4	30.00	4.6	-3.0	10.3	.513	.000	.069	.069	.026	.026
5	40.00	4.2	-3.0	10.2	.513	.000	.071	.071	.027	.027
6	50.00	3.8	-3.0	10.3	.514	.000	.074	.074	.027	.027
7	60.00	3.4	-3.0	10.6	.517	.000	.077	.077	.028	.028
8	70.00	3.0	-3.0	11.0	.522	.000	.081	.081	.029	.029
9	80.00	2.6	-3.0	11.8	.528	.000	.087	.087	.030	.030
10	90.00	2.3	-3.0	12.8	.537	.000	.096	.096	.032	.032
11	95.00	2.1	-3.0	13.5	.543	.000	.101	.101	.034	.034
HUB	100.00	1.8	-3.0	14.6	.552	.000	.109	.109	.036	.036

TABLE V.—BLADE GEOMETRY

(a) Inlet guide vane

RP	PERCENT SPAN	RADII RI	RADII RO	BLADE ANGLES KIC	BLADE ANGLES KTC	BLADE ANGLES KOC	DELTA INC	CONE ANGLE
TIP	0.	25.636	25.712	.00	.00	.00	11.70	.709
1	5.	25.065	25.147	.00	.00	.00	11.70	.766
2	10.	24.411	24.520	.00	.00	.00	11.69	1.019
3	20.	23.082	23.259	.00	.00	.00	11.68	1.651
4	30.	21.713	21.979	.00	.00	.00	11.66	2.472
5	40.	20.308	20.683	.00	.00	.00	11.64	3.490
6	50.	18.857	19.367	.00	.00	.00	11.60	4.730
7	60.	17.347	18.018	.00	.00	.00	11.55	6.216
8	70.	15.764	16.623	.00	.00	.00	11.49	7.951
9	80.	14.082	15.171	.00	.00	.00	11.40	10.033
10	90.	12.265	13.641	.00	.00	.00	11.26	12.598
11	95.	11.295	12.840	.00	.00	.00	11.16	14.085
HUB	100.	10.508	12.139	.00	.00	.00	11.09	14.834

RP	BLADE THICKNESSES TI	BLADE THICKNESSES TM	BLADE THICKNESSES TO	AXIAL DIMENSIONS ZI	AXIAL DIMENSIONS ZMC	AXIAL DIMENSIONS ZTC	AXIAL DIMENSIONS ZO
TIP	.123	.616	.062	-7.192	-4.729	-4.113	-1.035
1	.123	.616	.062	-7.192	-4.729	-4.114	-1.035
2	.123	.616	.062	-7.192	-4.729	-4.114	-1.036
3	.123	.616	.062	-7.192	-4.729	-4.113	-1.035
4	.123	.616	.062	-7.195	-4.732	-4.117	-1.039
5	.123	.617	.062	-7.195	-4.732	-4.117	-1.038
6	.124	.618	.062	-7.198	-4.735	-4.120	-1.041
7	.124	.619	.062	-7.202	-4.740	-4.125	-1.046
8	.124	.622	.062	-7.208	-4.746	-4.130	-1.052
9	.125	.625	.063	-7.215	-4.752	-4.137	-1.059
10	.126	.631	.063	-7.227	-4.764	-4.148	-1.070
11	.127	.635	.063	-7.235	-4.772	-4.156	-1.077
HUB	.128	.638	.064	-7.241	-4.778	-4.162	-1.084

RP	AERO CHORD	SETTING ANGLE	TOTAL CAMBER	SOLIDITY	TURNING RATIO	PHISS	CHOKE MARGIN
TIP	6.157	-.29	.00	.992	1.000	.00	.132
1	6.157	-.29	.00	1.015	1.000	.00	.130
2	6.157	-.29	.00	1.041	1.000	.00	.128
3	6.160	-.29	.00	1.100	1.000	.00	.119
4	6.161	-.29	.00	1.167	1.000	.00	.110
5	6.169	-.29	.00	1.245	1.000	.00	.102
6	6.178	-.29	.00	1.338	1.000	.00	.094
7	6.192	-.29	.00	1.449	1.000	.00	.088
8	6.215	-.29	.00	1.588	1.000	.00	.082
9	6.252	-.29	.00	1.769	1.000	.00	.077
10	6.309	-.29	.00	2.015	1.000	-.00	.074
11	6.348	-.29	.00	2.177	1.000	-.00	.075
HUB	6.369	-.29	.00	2.328	1.000	-.00	.076

TABLE V.—Continued.

(b) Rotor 1

RP	PERCENT SPAN	RADII RI	RO	BLADE ANGLES KIC	KTC	KOC	DELTA INC	CONE ANGLE
TIP	0.	25.613	24.973	64.13	60.20	49.27	2.97	-9.556
1	5.	25.057	24.468	62.69	58.89	48.63	3.20	-8.420
2	10.	24.444	23.963	61.22	57.51	47.85	3.44	-6.616
3	20.	23.229	22.952	58.73	54.88	45.72	3.93	-3.550
4	30.	22.008	21.941	56.48	51.41	43.25	4.41	-.800
5	40.	20.776	20.931	54.37	48.31	39.85	4.88	1.729
6	50.	19.520	19.920	52.33	45.34	35.29	5.34	4.186
7	60.	18.229	18.909	50.33	42.53	29.34	5.77	6.689
8	70.	16.889	17.899	48.33	39.61	22.00	6.13	9.324
9	80.	15.483	16.888	46.33	36.67	12.99	6.35	12.175
10	90.	13.993	15.877	44.33	33.78	1.70	6.33	15.336
11	95.	13.211	15.372	43.33	32.36	-5.09	6.19	17.060
HUB	100.	12.509	14.867	42.43	31.10	-11.85	6.06	18.117

RP	BLADE THICKNESSES TI	TM	TO	AXIAL DIMENSIONS ZI	ZMC	ZTC	ZO
TIP	.027	.222	.027	1.877	3.610	4.170	5.679
1	.028	.239	.028	1.778	3.600	4.097	5.755
2	.030	.257	.030	1.677	3.591	4.016	5.829
3	.036	.294	.036	1.506	3.577	3.841	5.974
4	.040	.331	.041	1.326	3.564	3.625	6.137
5	.044	.368	.045	1.159	3.549	3.383	6.293
6	.048	.407	.050	.994	3.529	3.116	6.454
7	.053	.447	.055	.825	3.503	2.814	6.622
8	.059	.490	.060	.642	3.471	2.480	6.793
9	.064	.537	.066	.446	3.436	2.119	6.959
10	.070	.589	.071	.229	3.396	1.719	7.099
11	.074	.618	.074	.108	3.372	1.504	7.151
HUB	.078	.645	.077	-.000	3.350	1.311	7.204

RP	AERO CHORD	SETTING ANGLE	TOTAL CAMBER	SOLIDITY	TURNING RATIO	PHISS	CHOKE MARGIN
TIP	7.584	59.56	14.86	1.336	.190	7.89	.075
1	7.595	58.16	14.07	1.367	.219	7.90	.067
2	7.590	56.71	13.36	1.397	.250	7.94	.061
3	7.580	53.94	13.01	1.463	.333	8.28	.064
4	7.577	50.73	13.23	1.536	.585	9.62	.080
5	7.578	47.48	14.52	1.619	.814	10.65	.086
6	7.585	43.95	17.05	1.714	.952	11.52	.088
7	7.600	39.98	20.99	1.824	.973	12.16	.085
8	7.628	35.34	26.33	1.954	.989	12.72	.083
9	7.678	29.94	33.34	2.114	.996	13.01	.080
10	7.760	23.49	42.64	2.316	1.002	12.83	.079
11	7.823	19.75	48.43	2.439	1.001	12.47	.079
HUB	7.885	16.05	54.28	2.567	1.000	12.15	.079

TABLE V.—Continued.

(c) Stator 1

RP	PERCENT SPAN	RADII RI	RO	BLADE ANGLES KIC	KTC	KOC	DELTA INC	CONE ANGLE
TIP	0.	24.846	24.826	37.03	21.26	-13.86	7.38	-.182
1	5.	24.362	24.336	37.31	21.78	-12.09	7.21	-.239
2	10.	23.876	23.879	37.58	22.20	-10.85	7.03	.057
3	20.	22.903	23.010	38.04	22.60	-10.22	6.62	1.029
4	30.	21.930	22.164	38.59	22.88	-10.06	6.20	2.353
5	40.	20.958	21.327	39.40	23.22	-10.15	5.78	3.833
6	50.	19.987	20.495	40.38	23.59	-10.47	5.35	5.489
7	60.	19.013	19.663	41.37	23.95	-10.93	4.92	7.282
8	70.	18.039	18.830	42.42	24.33	-11.54	4.50	9.216
9	80.	17.067	17.997	43.59	24.73	-12.38	4.08	11.257
10	90.	16.104	17.167	44.94	25.20	-13.44	3.67	13.380
11	95.	15.629	16.752	45.70	25.47	-14.01	3.47	14.445
HUB	100.	15.156	16.279	46.46	25.74	-14.66	3.26	14.787

RP	BLADE THICKNESSES TI	TM	TO	AXIAL DIMENSIONS ZI	ZMC	ZTC	ZO
TIP	.085	.527	.085	7.011	10.061	8.852	13.407
1	.081	.505	.081	7.083	10.063	8.905	13.345
2	.077	.484	.077	7.150	10.065	8.951	13.289
3	.071	.442	.070	7.266	10.072	9.012	13.189
4	.065	.402	.064	7.379	10.080	9.073	13.092
5	.058	.364	.059	7.494	10.090	9.138	12.999
6	.053	.329	.052	7.607	10.097	9.199	12.903
7	.047	.295	.047	7.720	10.104	9.255	12.808
8	.042	.263	.042	7.834	10.113	9.307	12.714
9	.037	.233	.037	7.948	10.123	9.358	12.622
10	.033	.204	.033	8.062	10.131	9.404	12.528
11	.030	.191	.030	8.121	10.136	9.428	12.483
HUB	.028	.177	.028	8.179	10.142	9.452	12.432

RP	AERO CHORD	SETTING ANGLE	TOTAL CAMBER	SOLIDITY	TURNING RATIO	PHISS	CHOKE MARGIN
TIP	6.527	11.59	50.89	1.422	1.000	20.32	.190
1	6.416	12.60	49.41	1.426	1.000	20.00	.191
2	6.308	13.36	48.43	1.430	1.000	19.75	.191
3	6.101	13.92	48.26	1.438	1.000	19.61	.184
4	5.899	14.30	48.64	1.448	1.000	19.61	.179
5	5.702	14.70	49.55	1.459	1.000	19.84	.176
6	5.508	15.06	50.85	1.472	1.000	20.19	.174
7	5.317	15.36	52.30	1.488	1.000	20.55	.171
8	5.132	15.64	53.96	1.506	1.000	20.95	.169
9	4.952	15.86	55.97	1.529	1.000	21.43	.168
10	4.776	16.07	58.38	1.554	1.000	22.03	.170
11	4.690	16.20	59.71	1.568	1.000	22.39	.172
HUB	4.582	16.30	61.11	1.577	1.000	22.74	.174

TABLE V.—Continued.

(d) Rotor 2

RP	PERCENT SPAN	RADII RI	RO	BLADE ANGLES KIC	KTC	KOC	DELTA INC	CONE ANGLE
TIP	0.	24.778	24.300	63.49	54.90	46.37	3.35	-8.299
1	5.	24.307	23.868	61.92	53.79	45.88	3.64	-7.345
2	10.	23.867	23.504	60.51	52.77	45.40	3.92	-5.895
3	20.	23.025	22.800	58.15	50.89	44.17	4.46	-3.478
4	30.	22.201	22.110	56.40	49.13	42.43	4.97	-1.351
5	40.	21.390	21.433	54.91	47.30	40.06	5.47	.610
6	50.	20.581	20.765	53.48	45.47	37.09	5.96	2.505
7	60.	19.773	20.107	52.11	43.53	33.48	6.43	4.367
8	70.	18.966	19.462	50.81	41.51	29.22	6.88	6.218
9	80.	18.161	18.835	49.63	39.37	24.01	7.30	8.087
10	90.	17.355	18.230	48.67	36.98	16.95	7.64	9.992
11	95.	16.950	17.937	48.30	35.61	12.43	7.78	10.961
HUB	100.	16.487	17.556	47.87	34.05	6.70	7.94	11.527

RP	BLADE THICKNESSES TI	TM	TO	AXIAL DIMENSIONS ZI	ZMC	ZTC	ZO
TIP	.028	.201	.027	14.275	15.749	16.341	17.549
1	.030	.219	.030	14.201	15.745	16.279	17.603
2	.032	.236	.032	14.136	15.743	16.221	17.647
3	.037	.268	.038	14.029	15.741	16.103	17.729
4	.042	.300	.042	13.941	15.737	15.979	17.806
5	.046	.331	.047	13.859	15.732	15.849	17.888
6	.051	.362	.051	13.778	15.727	15.711	17.976
7	.055	.393	.056	13.697	15.721	15.564	18.070
8	.059	.425	.061	13.611	15.710	15.405	18.166
9	.064	.457	.065	13.520	15.698	15.237	18.270
10	.069	.490	.070	13.414	15.681	15.048	18.384
11	.071	.506	.072	13.349	15.665	14.941	18.443
HUB	.074	.525	.074	13.275	15.647	14.820	18.519

RP	AERO CHORD	SETTING ANGLE	TOTAL CAMBER	SOLIDITY	TURNING RATIO	PHISS	CHOKE MARGIN
TIP	5.962	56.43	17.12	1.237	.470	13.37	.153
1	5.968	55.08	16.04	1.262	.537	13.08	.139
2	5.964	53.87	15.11	1.282	.601	12.85	.128
3	5.958	51.71	13.98	1.324	.724	12.64	.119
4	5.955	49.70	13.97	1.369	.843	12.90	.117
5	5.955	47.61	14.85	1.416	.935	13.42	.117
6	5.958	45.36	16.39	1.468	.972	13.93	.118
7	5.962	42.85	18.63	1.523	.989	14.51	.119
8	5.970	40.08	21.58	1.582	.997	15.14	.121
9	5.983	36.91	25.62	1.647	1.001	15.87	.126
10	6.000	32.96	31.72	1.718	1.000	16.89	.139
11	6.013	30.55	35.87	1.756	1.000	17.56	.150
HUB	6.025	27.52	41.18	1.803	1.000	18.32	.162

TABLE V.—Continued.

(e) Stator 2

RP	PERCENT SPAN	RADII RI	RO	BLADE ANGLES KIC	KTC	KOC	DELTA INC	CONE ANGLE
TIP	0.	24.206	24.193	40.01	20.69	-14.97	8.10	-.177
1	5.	23.798	23.785	38.86	21.01	-12.63	7.91	-.177
2	10.	23.451	23.459	38.04	21.22	-11.16	7.74	.111
3	20.	22.778	22.837	37.26	21.36	-10.20	7.35	.841
4	30.	22.121	22.236	37.73	21.78	-9.83	6.94	1.671
5	40.	21.472	21.648	38.75	22.32	-9.76	6.53	2.590
6	50.	20.831	21.074	39.83	22.83	-9.89	6.12	3.624
7	60.	20.196	20.512	40.91	23.36	-10.18	5.71	4.769
8	70.	19.573	19.964	42.08	23.86	-10.66	5.31	5.971
9	80.	18.962	19.430	43.41	24.37	-11.41	4.92	7.236
10	90.	18.367	18.917	45.18	24.99	-12.55	4.53	8.597
11	95.	18.076	18.671	46.33	25.35	-13.29	4.34	9.342
HUB	100.	17.706	18.308	47.75	25.80	-14.33	4.09	9.535

RP	BLADE THICKNESSES TI	TM	TO	AXIAL DIMENSIONS ZI	ZMC	ZTC	ZO
TIP	.069	.384	.069	18.985	20.929	20.321	23.094
1	.067	.371	.067	19.003	20.932	20.308	23.075
2	.065	.359	.065	19.016	20.934	20.298	23.059
3	.060	.336	.060	19.036	20.935	20.280	23.032
4	.057	.315	.056	19.068	20.937	20.292	23.010
5	.053	.294	.052	19.099	20.936	20.312	22.987
6	.049	.274	.049	19.133	20.939	20.335	22.969
7	.046	.255	.046	19.164	20.940	20.349	22.949
8	.042	.236	.042	19.194	20.940	20.363	22.930
9	.039	.218	.039	19.225	20.941	20.377	22.913
10	.036	.201	.036	19.259	20.942	20.392	22.899
11	.035	.194	.035	19.277	20.943	20.403	22.893
HUB	.033	.183	.033	19.300	20.943	20.416	22.884

RP	AERO CHORD	SETTING ANGLE	TOTAL CAMBER	SOLIDITY	TURNING RATIO	PHISS	CHOKE MARGIN
TIP	4.208	12.55	54.98	1.273	1.000	24.86	.280
1	4.179	13.11	51.49	1.286	1.000	23.23	.259
2	4.155	13.44	49.20	1.297	1.000	22.04	.244
3	4.108	13.54	47.47	1.319	1.000	20.77	.226
4	4.063	13.97	47.56	1.341	1.000	20.55	.219
5	4.019	14.53	48.51	1.365	1.000	20.80	.218
6	3.978	15.01	49.72	1.390	1.000	21.09	.217
7	3.938	15.43	51.09	1.417	1.000	21.41	.215
8	3.902	15.80	52.73	1.445	1.000	21.80	.214
9	3.868	16.12	54.82	1.475	1.000	22.35	.215
10	3.837	16.46	57.74	1.507	1.000	23.27	.223
11	3.824	16.69	59.61	1.524	1.000	23.94	.232
HUB	3.797	16.92	62.09	1.544	1.000	24.77	.242

TABLE V.—Continued.

(f) Rotor 3

RP	PERCENT SPAN	RADII RI	RO	BLADE ANGLES KIC	KTC	KOC	DELTA INC	CONE ANGLE
TIP	0.	24.183	23.769	64.76	49.81	42.83	3.65	-8.673
1	5.	23.772	23.410	62.36	49.41	42.78	4.04	-7.356
2	10.	23.441	23.147	60.59	49.07	42.68	4.34	-5.847
3	20.	22.826	22.640	58.05	48.28	42.10	4.91	-3.579
4	30.	22.240	22.146	56.39	47.29	40.85	5.44	-1.744
5	40.	21.671	21.666	55.04	46.12	39.09	5.96	-.083
6	50.	21.116	21.194	53.80	44.84	37.00	6.45	1.374
7	60.	20.573	20.735	52.68	43.44	34.50	6.93	2.758
8	70.	20.042	20.290	51.67	41.95	31.57	7.39	4.100
9	80.	19.525	19.861	50.78	40.27	27.90	7.82	5.368
10	90.	19.024	19.454	50.06	38.24	22.79	8.20	6.608
11	95.	18.780	19.261	49.78	37.01	19.47	8.37	7.227
HUB	100.	18.420	18.951	49.35	35.24	14.32	8.62	7.721

RP	BLADE THICKNESSES TI	TM	TO	AXIAL DIMENSIONS ZI	ZMC	ZTC	ZO
TIP	.028	.176	.028	24.234	25.417	25.938	26.948
1	.031	.194	.031	24.170	25.418	25.883	26.975
2	.033	.208	.033	24.124	25.419	25.839	26.995
3	.038	.235	.038	24.057	25.422	25.761	27.032
4	.042	.261	.041	24.008	25.425	25.688	27.075
5	.045	.286	.046	23.964	25.428	25.615	27.126
6	.050	.310	.050	23.919	25.429	25.537	27.177
7	.053	.334	.053	23.877	25.431	25.459	27.235
8	.057	.357	.057	23.833	25.431	25.376	27.294
9	.061	.380	.061	23.784	25.427	25.285	27.359
10	.064	.403	.065	23.724	25.420	25.182	27.437
11	.066	.414	.066	23.687	25.413	25.122	27.480
HUB	.069	.430	.069	23.634	25.403	25.037	27.549

RP	AERO CHORD	SETTING ANGLE	TOTAL CAMBER	SOLIDITY	TURNING RATIO	PHISS	CHOKE MARGIN
TIP	4.629	53.79	21.92	1.198	1.000	20.10	.257
1	4.631	52.54	19.57	1.218	1.000	18.38	.210
2	4.628	51.62	17.91	1.233	1.000	17.17	.180
3	4.622	50.06	15.95	1.262	1.000	15.82	.158
4	4.620	48.61	15.54	1.292	1.000	15.49	.151
5	4.620	47.07	15.95	1.324	1.000	15.59	.149
6	4.620	45.41	16.80	1.356	1.000	15.84	.148
7	4.622	43.60	18.19	1.389	1.000	16.28	.151
8	4.624	41.64	20.10	1.423	1.000	16.84	.155
9	4.628	39.38	22.88	1.459	1.000	17.61	.163
10	4.633	36.50	27.27	1.495	1.000	18.78	.180
11	4.636	34.70	30.31	1.513	1.000	19.59	.192
HUB	4.643	31.92	35.04	1.542	1.000	20.74	.209

TABLE V.—Concluded.

(g) Stator 3

RP	PERCENT SPAN	RADII RI	RO	BLADE ANGLES KIC	KTC	KOC	DELTA INC	CONE ANGLE
TIP	0.	23.680	23.660	40.15	20.05	-15.73	8.81	-.354
1	5.	23.337	23.323	38.99	20.54	-13.11	8.59	-.255
2	10.	23.086	23.086	38.26	20.82	-11.65	8.42	.057
3	20.	22.607	22.639	37.54	21.02	-10.67	8.04	.569
4	30.	22.137	22.210	38.26	21.56	-10.28	7.63	1.271
5	40.	21.679	21.793	39.40	22.17	-10.20	7.22	1.995
6	50.	21.226	21.388	40.48	22.71	-10.30	6.81	2.844
7	60.	20.784	20.993	41.55	23.25	-10.57	6.42	3.699
8	70.	20.352	20.611	42.65	23.73	-11.03	6.03	4.573
9	80.	19.935	20.246	43.83	24.19	-11.76	5.66	5.484
10	90.	19.535	19.898	45.25	24.66	-12.83	5.29	6.414
11	95.	19.340	19.732	46.11	24.91	-13.48	5.11	6.922
HUB	100.	19.040	19.441	47.40	25.29	-14.58	4.83	7.098

RP	BLADE THICKNESSES TI	TM	TO	AXIAL DIMENSIONS ZI	ZMC	ZTC	ZO
TIP	.069	.343	.069	28.166	29.726	29.267	31.460
1	.066	.332	.066	28.169	29.726	29.248	31.453
2	.065	.324	.065	28.170	29.726	29.235	31.450
3	.062	.309	.061	28.171	29.728	29.216	31.448
4	.059	.294	.058	28.178	29.727	29.221	31.447
5	.056	.279	.056	28.187	29.725	29.231	31.447
6	.053	.265	.053	28.196	29.724	29.239	31.448
7	.050	.251	.050	28.205	29.724	29.243	31.449
8	.047	.237	.047	28.214	29.725	29.248	31.453
9	.045	.224	.045	28.221	29.725	29.250	31.456
10	.043	.211	.042	28.229	29.724	29.252	31.460
11	.041	.205	.041	28.234	29.724	29.255	31.462
HUB	.039	.196	.039	28.243	29.723	29.260	31.466

RP	AERO CHORD	SETTING ANGLE	TOTAL CAMBER	SOLIDITY	TURNING RATIO	PHISS	CHOKE MARGIN
TIP	3.368	12.23	55.88	1.223	1.000	26.25	.320
1	3.368	12.94	52.10	1.241	1.000	24.43	.296
2	3.368	13.30	49.91	1.254	1.000	23.26	.280
3	3.368	13.44	48.21	1.279	1.000	21.94	.262
4	3.368	14.00	48.54	1.305	1.000	21.87	.256
5	3.369	14.62	49.60	1.332	1.000	22.17	.257
6	3.371	15.12	50.78	1.360	1.000	22.46	.256
7	3.372	15.54	52.12	1.387	1.000	22.76	.255
8	3.376	15.87	53.68	1.417	1.000	23.11	.255
9	3.381	16.10	55.60	1.446	1.000	23.57	.256
10	3.386	16.30	58.08	1.476	1.000	24.29	.263
11	3.388	16.41	59.58	1.490	1.000	24.78	.269
HUB	3.387	16.55	61.98	1.513	1.000	25.51	.277

TABLE VI.—MECHANICAL DESIGN PARAMETERS

Blade row	Blade stress factor of safety	Bending flutter parameter	Torsion flutter parameter
Rotor 1	1.98	2.73	0.88
Rotor 2	2.80	2.32	.89
Rotor 3	3.74	2.01	.87
Stator 1	20.37	2.11	1.06
Stator 2	15.80	1.91	.92
Stator 3	14.15	1.46	.75

1. Report No. NASA TP-2597	2. Government Accession No.	3. Recipient's Catalog No.
4. Title and Subtitle Design of 9.271-Pressure-Ratio Five-Stage Core Compressor and Overall Performance for First Three Stages		5. Report Date May 1986
		6. Performing Organization Code 505-62-21
7. Author(s) Ronald J. Steinke		8. Performing Organization Report No. E-2589
		10. Work Unit No.
9. Performing Organization Name and Address National Aeronautics and Space Administration Lewis Research Center Cleveland, Ohio 44135		11. Contract or Grant No.
		13. Type of Report and Period Covered Technical Paper
12. Sponsoring Agency Name and Address National Aeronautics and Space Administration Washington, D.C. 20546		14. Sponsoring Agency Code

15. Supplementary Notes

16. Abstract

Overall aerodynamic design information is given for all five stages of an axial flow core compressor (74A) having a 9.271 pressure ratio and 29.710 kg/sec flow. For the inlet stage group (first three stages), detailed blade element design information and experimental overall performance are given. At rotor 1 inlet tip speed was 430.291 m/sec, and hub to tip radius ratio was 0.488. A low number of blades per row was achieved by the use of low-aspect-ratio blading of moderate solidity. The high reaction stages have about equal energy addition. Radial energy varied to give constant total pressure at the rotor exit. The blade element profile and shock losses and the incidence and deviation angles were based on relevant experimental data. Blade shapes are mostly double circular arc. Analysis by a three-dimensional Euler code verified the experimentally measured high flow at design speed and IGV-stator setting angles. An optimization code gave an optimal IGV-stator reset schedule for higher measured efficiency at all speeds.

17. Key Words (Suggested by Author(s)) Compressor design; Axial flow compressor; Multistage compressor	18. Distribution Statement Unclassified - unlimited; STAR Category 07

19. Security Classif. (of this report)	20. Security Classif. (of this page)	21. No. of pages	22. Price*
Unclassified	Unclassified	34	A03

*For sale by the National Technical Information Service, Springfield, Virginia 22161

NASA-Langley, 1986